Surfaces and Interfaces 26 (2021) 101444

Contents lists available at ScienceDirect

Surfaces and Interfaces

journal homepage: www.sciencedirect.com/journal/surfaces-and-interfaces

Surface tension and viscosity–temperature dependence and mutual causal correlation in tin-silver alloys

Rachida M'chaar [a], Noureddine Ouerfelli [b], Mehrzia Krimi Ammar [c], Baraa Hafez [d], Man Singh [e], Aymen Messaâdi [b], Hicham Elmsellem [f,*], Hüseyin Arslan [g,h]

[a] Center of Water, Natural Resources, Environment and Sustainable Development, Laboratory of Spectroscopy, Molecular Modeling, Materials, Nanomaterials, Water and Environment, CERNE2D, Mohammed V University in Rabat, Faculty of Sciences, Av. Ibn Battouta, B.P. 1014 Rabat, Morocco
[b] Université de Tunis El Manar, Laboratoire Biophysique et de Technologies Médicales LR13ES07, Institut Supérieur des Technologies Médicales de Tunis, 9 Avenue Dr. Zouhaier Essafi 1006 Tunis, Tunisie
[c] Université de Tunis El Manar, Laboratoire des Matériaux et de l'Environnement pour le Développement Durable, LR18ES10, 9 Avenue Dr. Zouhaier Essafi 1006 Tunis, Tunisia
[d] Department of Pharmaceutical Sciences, College of Pharmacy and Health Sciences, Ajman University, PO Box 346, Ajman, UAE
[e] School of Chemical Sciences, Central University of Gujarat, Gandhinagar 382030, India
[f] Laboratoire de chimie appliquée et environnement (LCAE), Faculté des Sciences, B.P. 717, 60000 Oujda, Morocco
[g] Faculty of Science and Letters, Department of Physics, Kahramanmaras Sutcuimam University, Onikisubat Kahramanmaras, Turkey
[h] Institute for Graduate Studies in Science and Technology, Department of Material Science and Engineering, Kahramanmaras Sutcuimam University, Onikisubat Kahramanmaras, Turkey

ARTICLE INFO

Keywords:
Surface tension
Viscosity
Ag-Sn
Arrhenius behavior
Friccohesity
Gibbs free energy
Modeling

ABSTRACT

Thermo-physical properties for binary and multi-components alloys are important for controlling and designing metallurgical processes. However, it is difficult to get data from systems of a high order in terms of experience. On the theoretical level, different formalisms have been adopted for determining the structural, transport, and electronic properties, therefore, most thermo-physical data from calculations theoretical. Indeed, to choose the best substitute alloy, many criteria must be taken into account, in particular the surface tension, density, viscosity, and friccohesity. The Sn-Ag binary alloy is one of the most common lead-free solders. It is characterized by more interesting thermo-physical properties. In the present work, we have suggested novel empirical expressions of these physicochemical properties against the temperature where the corresponding obtained optimal coefficients are expressed with mole composition of tin which permit us to combine the two dependences and propose unified equations correlating thermophysical properties of the alloy as the function of both the independent variables the temperature and composition.

1. Introduction

The study and development of materials, one of the oldest areas of human research, now called "functional Materials Science", has made it possible to design and to produce products for increasingly specific uses. In one particular field, that of metal alloys, it is not uncommon to find commercial alloys in several fields of modern industry. One of the applications of metal alloys is welds, in particular in the electronics industry requiring alloys which melt at low temperature (below 250°C).

Replacement of lead in alloys used for soldering in industry microelectronics is the subject of a global economic and strategic challenge. The harmfulness of lead is known. In low doses, its ingestion causes disorders neurological or birth defects. In high doses, this element causes poisoning of the organism. Risk is limited for user's electronic circuits at temperatures close to ambient. However, the alloys conventional lead-based landfills can pollute groundwater. Personnel handling electronic circuits at high temperatures and large quantities are also at risk. A few years after the legislation of July 1, 2006 [1] decided on the main deadlines for replace lead in solder alloys, demand remains imprecise, and no standard can completely replace the tin / lead eutectic (traditional solder). The basic element of the replacement alloy remains tin which has a relatively low melting point (232°C), but 50°C higher

"This article is dedicated to our Dear Professor Mohamed LFERDE Ex-Professor at the Mohammed V University in Rabat, Faculty of Sciences, Morocco

* Corresponding author.
E-mail address: h.elmsellem@gmail.com (H. Elmsellem).

https://doi.org/10.1016/j.surfin.2021.101444
Received 7 May 2021; Received in revised form 26 July 2021; Accepted 25 August 2021
Available online 4 September 2021

than the eutectic Sn-Pb (183°C) and which is the majority common element in new alloys of welding. Other elements, combined with this element, can replace lead. At the level of a tin matrix, several alloys have been developed and some of them have been studied, in particular within the framework of the European project COST531 "Lead Free Solders" [2]. Indeed, replacing lead with bismuth or indium is unthinkable given the low levels of limited reserves. Despite the interest that present these two elements, their use is limited and therefore they cannot intervene as minor elements in new welds. To choose the best substitute alloy, many criteria must be taken into account, in particular the density, surface tension, viscosity, and friccohesity. The Sn-Ag binary alloy is one of the most common lead-free solders. It is characterized by more interesting thermo-physical properties. Many research studies have used different methods to determine the thermo-physical properties of Ag-Sn liquid alloys *vs*. the temperature and composition.

The surface tension for Ag-Sn alloys in the liquid state has been the subject of several research studies, first in 1961 with Lauerman *et al.* [3], then by Vincent *et al.* [4] in 1993. The work of Moser *et al.* [5] published in 2001 presented two methods for measuring the surface tension of pure tin and binary alloys Sn-Ag. These authors observed a linear dependence of the surface tension for these alloys *vs*. temperature. Recently, Lee *et al.* [6] experimentally determined the surface tension of liquid alloys Sn-Ag and Sn-Cu by the drop method for a temperatures interval ranging from 700 K to 1500 K. The results obtained show that the surface tension increases with the amount of silver added and as the coefficient of temperature ($d\sigma/dT$) had both positive and negative values. Recently, other authors [7–13] have measured the surface tension of alloys binary Sn-Ag in liquid state by different methods. The lack of viscosity experimental data of an alloy constitutes a major constraint in research. Works by Gebhardt et *al.* [14] have been the subject of several publications studying the viscosity of pure tin and Sn-Ag alloys in the liquid state. Complementary work by Gancarz et *al.* [13], focused on a study the viscosity of pure tin and Sn-Ag alloys in the liquid state. These authors [13] have also shown that the viscosity of pure tin and Sn-Ag alloys decreases logarithmically with increasing temperature and data obtained were interpreted using an Arrhenius-type equation.

Within our Laboratory, several works have been published as part of the development and the thermo-physical study of lead-free ternary, quaternary, and quinary alloys [13–24]. Obtaining such information through techniques is heavy and expensive. Prediction of thermo-physical properties involving liquid solutions plays an important role in the development and understanding of metallurgical processes. The growth importance of digital process simulation metallurgical forces to establish thermo-physical models that give better estimations of thermo-physicochemical properties with unique friccohesity chemistry.

In the present work, we aim to present interesting new models correlating some physicochemical properties, such as molar volume, surface tension, density, viscosity [25–30] and the new concept of friccohesity [31–35] for the {Sn (1) + Ag (2)} binary alloys *vs*. the molar fraction (x_1) of Sn through the interval of temperature (623.15 to 1223.15) K. The friccohesity (s/cm = second/cm) and friccohesity chemistry become a most sensitive operator to predict homogeneous mixing of the Sn with its increasing compositions within the Sn-Ag networking or leading to cluster around the already present Sn. Such clustering of adding Sn increases the cohesive forces with higher surface tension and decreasing the shear stress or the viscosity. However, there could also be the possibility that the Sn could get distributed around the caging of the Ag in such situation the shear increases, and the surface tension decreases. Therefore, the overall engineering of the Sn-Ag networking could be elaborated and elucidated by analyzing the data of the friccohesity. The electronic configuration of the Sn and Ag on their interactive model at Bohr radius intermix their wave function which is of most sensitive quantum mechanics of these metallic atoms which is explained with following quantum mechanics equation.

$$r_B = \frac{n^2h^2}{4\pi^2me^2} \times \frac{1}{Z}$$

The r_B is Bohr radius in nanometer (nm) of Sn and Ag metallic atoms, Z is their atomic numbers, n is their principal quantum numbers, h is Planck constant, m electron mass, e is electron charge. Hence it is unavoidable that their electronic clouds with specific wave functions intermix and sense the wave functions of the similar atoms or the dissimilar atom. Because the combinations of the similar atoms in the Sn + Ag cluster increase cohesive forces while the Sn homogenization affect the viscosity. The friccohesity (ϕ_h) is determined using Mansingh equation noted as under.

$$\varphi_h = M_c[(t \times n)]$$

Where ($M_c = \frac{\varphi_{h0}}{t_0 n_0}$) represents the Mansingh constant.

The ϕ_h, is friccohesity of sample, ϕ_{h0} is friccohesity of base material noted as medium, t_0 and n_0 are the viscous flow time and the pendant drop numbers of base material, t and n are the viscous flow time and the pendant drop numbers of sample. These are the reasons that the friccohesity chemistry has become the most relevant chemistry of these studies to predict the homogenization of the Sn in the Sn + Ag material. Therefore, the friccohesity sense such reorientation of the metallic alignments induces of clustering of the similar atoms or the different atoms. Hence, the similar atoms adherence or the different atom adherence together truly generates a most advanced friccohesity chemistry to understand the hardcore chemistry of the metallic combinatorial engineering to develop the metallic products. The friccohesity vary with increasing temperature is calculated as:

$$\varphi_h = M_C^0 \pm S_{t.n} \times T$$

The M_c^0 isthe limiting friccohesity constant, $S_{t.n}$ is slope values, and T is the absolute temperature in Kelvin.

2. Semi-empirical modeling of temperature's parameters in binary tin-silver alloys

In the literature, experimenters present numerical values of the temperature effect, generally in linear dependence, in Tables for well-determined temperatures and compositions of their studied mixture. Lee et *al.* [6] experimentally determined the surface tension of liquid alloys Sn-Ag binary alloys by the drop method for an interval temperature ranging from 700 K to 1500 K. The results obtained show that the surface tension increases with the amount of silver added and as the coefficient of temperature ($d\sigma/dT$) had both positive and negative values. Moser et *al.* [8] obtained negative values for the coefficient of temperature of the Ag-Sn alloy. The results of Lee et *al.* [6] also show a significant dependence between temperature and surface tension. Indeed, when the temperature increases, the surface tension for pure silver decreases, which gives a negative value of the coefficient $d\sigma/dT$. The work of Gancarz et *al.* [9] published in 2011 presented two methods for measuring the surface tension of pure tin and binary alloys Sn-Ag: The Roach-Henein (RH) method in the 655-1255K temperature range. The second method is the one that uses the Butler equation [36]. These authors observed a linear dependence of the surface tension for these alloys *vs*. temperature. Their measurements were compared with the values calculated by the equation of Butler [37]. They observed a good agreement between the values calculated with those found experimentally. However, there is always the scope to initiate the creative models and the approaches for the better interpretations and the explorations such as friccohesity study.

In this case, the need arises for modeling the temperature parameters for predicting its values at other untreated temperatures and compositions in these literatures as well as for generalization to multi-constituent alloys requiring knowledge of the data of the pure constituents and their binary alloys, etc. The purpose of this work is to expose

certain semi-empirical expressions of temperature coefficients to different compositions of the Sn-Ag binary alloys. For this, we started from experimental data of surface tension, density and dynamic viscosity reported from three works in the literature [9,14,37] for Sn-Ag binary alloys at different compositions and temperatures.

Nevertheless, we notice that these three properties have not the same studied molar compositions while our goal in the present work is to use these properties to determine interesting new derived properties and features, such as the Arrhenius temperature, the apparent friccohesity, the viscosity of the saturated vapor, etc.., also for some estimations and predictions, like the normal boiling temperature of the pure metals or of its binary mixtures. In addition, we record few molar compositions that have been studied in these works [25–30], which results in low performance of mathematical regressions and simulations, etc. Due to the constraints of the small number of points provided by the literature and the need for mathematical handlings of continuity and derivations, we have used general and/or local interpolation and extrapolation methods to ensure continuity and first and second derivability, and fitted in polynomial of adequate degrees with least-squares optimization method to afforded eighteen data points against common molar composition x_1 of tin in Sn-Ag binary liquid alloys at the seven common temperatures from 623.15 K to 1223.15K (Tables S1-S3 and Figures S1-S3 in Supplementary Materials). Moreover, the unification of molar fractions, and the expansion by addition of some intermediate data to obtain experimental and calculated data points uniformly distributed throughout the whole range of molar composition by using some local interpolations for mathematical derivations, are necessary especially for well describe some cluster or complex formation, or structure breaking and eutectic, manifested by the apparition of some singular points in certain curves during graphical representation of some derived properties.

2.1. Surface tension

The plot of the surface tension with temperature at given composition exhibit generally a linear behavior [9,14,37] and obeys the following equation:

$$\sigma = a\sigma 0 + a\sigma 1 \times T \tag{1}$$

Where $a_{\sigma 0}$ and $a_{\sigma 1}$ are optimal coefficients independent of temperature and depending on the molar composition (x_1) of the given Sn-Ag binary alloy.

In fact, Figure S4 clearly shows the quasi-perfect linear dependence with temperature and permits us to determinate values of temperature parameters which are presented in Table 1.

A rapid dimensional analysis equation shows that the parameter ($a_{\sigma 0}$) is the limit of the surface tension when the absolute temperature rends to the zero and it can be symbolized by (σ_0). As well, the parameter ($a_{\sigma 1}$) it the derivative of the surface tension with respect to the absolute temperature (T) at constant pressure P Eq. (2).

$$\begin{cases} a_{\sigma 0} = \lim\limits_{T\to 0}\sigma \\ a_{\sigma 1} = \left(\dfrac{\partial\sigma}{\partial T}\right)_P \end{cases} \tag{2}$$

In addition, considering that the surface energy corresponds to the excess free energy (ΔG) that must be supplied to the area Ω of a given surface, to increase it by an increment (or increase) dΩ (Eq. 3), taking into account the need to rebalance the surface atomic bonds and assuming that the temperature, the volume of the solid and the number of constituents (within the meaning of the phase rule) remain constant [38,39].

$$\begin{cases} \sigma = -\left(\dfrac{\partial\Delta G}{\partial\Omega}\right)_{T,P,x_i} \\ \Delta G = \Delta H - T\Delta S \\ \Delta S = -\left(\dfrac{\partial\Delta G}{\partial T}\right)_P \end{cases} \tag{3}$$

Where ΔH and ΔS are the entropy and entropy, respectively. Combining Eqs. 2 and 3, and considering ΔG, ΔH and ΔS are exact total differential thermodynamic functions; we can conclude that the parameter ($a_{\sigma 1}$) is equivalent to the opposite of surface entropy (S_σ). So, the Eq. 1 becomes a semi-empirical one expressed as follows:

$$\sigma = \sigma 0 - S\sigma \times T \tag{4}$$

Values of the limiting surface tension (σ_0) and surface entropy (S_σ) are presented in Table 1 and depicted in Figs. 1 and 2. Regarding the previous discussion and the dimension (Table 1), we can also consider that (S_σ) can represent an energy density per unit area. Figs. 1 and 2 show an interesting minimum around the molar fraction on tin equivalent to 0.4. Given that the surface entropy (S_σ) is in correlation with the disorder between atoms, we can conclude that this particular composition is equivalent to the cluster (Ag_3Sn_2) where there is a weakening of cohesion and friction between metal atoms in liquid state and the temperature effect is negligible (Figure S1). We add that an inspection of the eventual causal correlation between the two temperature parameters (σ_0) and (S_σ) we have plotted in Fig. 3 the ratio (σ_0/S_σ) which is equivalent to a specific temperature (T_σ) in relationship to the thermal

Table 1
Parameters values of Eqs. 1 and 4, and specific temperature (T_σ) for the {Sn (1) + Ag (2)} systems *vs.* the molar fraction (x_1) of Sn through the interval of temperature (623.15 to 1223.15) K.

$x_1 = x_{Sn}$ -	$a_{\sigma 0} = \sigma_0$ $N.m^{-1}$	$a_{\sigma 1} = -S_\sigma$ $\mu N{\cdot}K^{-1}{\cdot}m^{-1}$ or $\mu J{\cdot}K^{-1}{\cdot}m^{-2}$	R -	$T_\sigma \times 10^{-3}$ K
0.000	1.1489	-197.50	1	5.8172
0.0686	1.0164	-143.68	0.99990	7.0741
0.1000	0.96790	-127.78	1	7.5747
0.1500	0.91119	-112.00	1	8.1356
0.2500	0.78011	-71.214	0.99998	10.954
0.3000	0.71700	-52.000	1	13.788
0.3529	0.65350	-34.989	1	18.677
0.4000	0.61292	-14.000	1	43.780
0.4761	0.59947	-26.000	0.99933	23.057
0.5000	0.60062	-33.400	1	17.983
0.6000	0.61194	-58.000	1	10.551
0.7000	0.62100	-78.321	0.99999	7.9289
0.7500	0.62596	-89.000	1	7.0333
0.8200	0.61833	-92.036	0.99998	6.7183
0.8780	0.60094	-88.000	1	6.8289
0.9000	0.59660	-88.286	0.99999	6.7576
0.9620	0.58598	-90.000	1	6.5109
1.000	0.59632	-89.775	1	6.6424

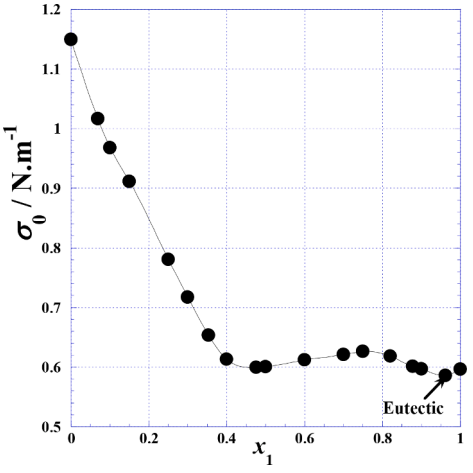

Fig. 1. Limiting surface tension (σ_0) for the {Sn (1) + Ag (2)} systems *vs.* the mole fraction (x_1) of Sn through the interval of temperature (623.15 to 1223.15) K.

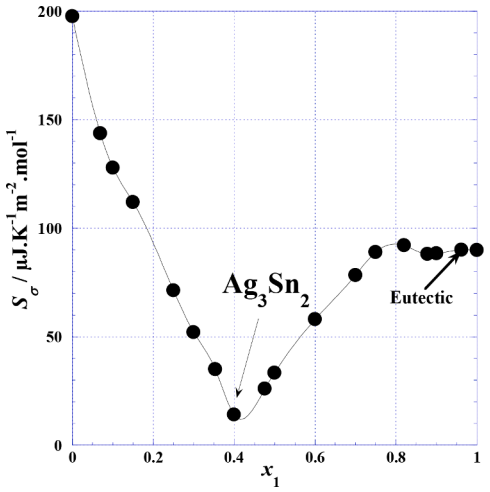

Fig. 2. Surface entropy (S_σ) for the {Sn (1) + Ag (2)} systems *vs.* the molar fraction (x_1) of Sn through the interval of temperature (623.15 to 1223.15) K.

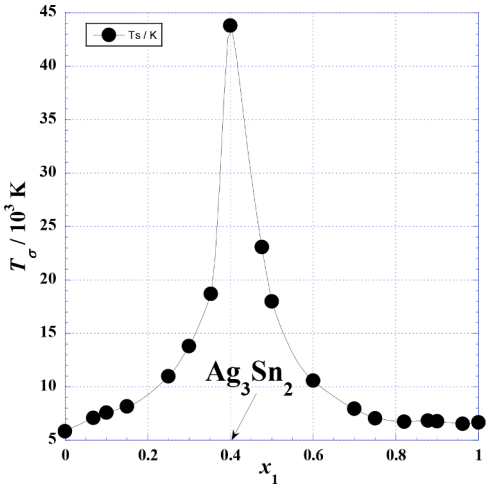

Fig. 3. Specific temperature (T_σ) for the {Sn (1) + Ag (2)} systems *vs.* the molar fraction (x_1) of Snthrough the interval of temperature (623.15 to 1223.15) K.

agitation in connection to the surface phenomena such as friction, cohesion forces, viscosity and friccohesity [29–35]. The value of this specific temperature (T_σ) is an interesting criterion of the intensity of the interatomic forces in the free surface of liquid binary alloy.

Joining the scatter points by smoothing or interpolation in Figs. 1 and 2 facilitates manually to give other extracted coordinates using any graphic software or local interpolation which permit to estimate or predict new other data with different temperatures or molar compositions necessary for specific personal experiments or for generalization to ternary or multi-components alloys systems. Finally, hope this modeling of temperature parameters and graphical behaviors; contribute on the improvement and development of some theories previously available to advance the science and technology of the eutectics.

2.2. Density and molar volume

The density of pure tin and Sn-Ag binary alloys was initially studied in 2001 by Moser et *al.* [5], they used the dilatometric technique to determine over a range of temperatures from 500 K to 1400 K and have shown that the density increases linearly with temperature, and this for all concentrations of the studied tin.

The plot of the density with temperature at given composition exhibit generally a linear behavior [5] and obeys the following equation:

$$\rho = a\rho 0 + a\rho 1 \times T \tag{5}$$

Where $a_{\rho 0}$ and $a_{\rho 1}$ are optimal coefficients independent of temperature and depending on the molar composition (x_1) of the given Sn-Ag binary alloy.

In fact, Fig. S5 clearly shows the quasi-perfect linear dependence with temperature and permits us to determinate values of temperature parameters ($a_{\rho 0}$ and $a_{\rho 1}$) which are presented in Table 2.

A rapid dimensional analysis equation shows that the parameter ($a_{\rho 0}$) is the limit of the density when the absolute temperature rends to the zero and it can be symbolized by (ρ_0). As well, the parameter ($a_{\rho 1}$) it the derivative of the density with respect to the absolute temperature (T) at constant pressure P (Eq. 6).

$$\begin{cases} a_{\rho 0} = \lim\limits_{T\to 0}\rho = \rho_0 \\ a_{\rho 1} = \left(\dfrac{\partial \rho}{\partial T}\right)_P = -\alpha\cdot\rho \end{cases} \tag{6}$$

Where (α) is the isobaric thermal expansion expressed as follows:

$$\alpha(x_1, T) = -\frac{1}{\rho(x_1, T)}\cdot\left(\frac{\partial \rho(x_1, T)}{\partial T}\right)_P \tag{7}$$

Considering the Eqs. 5–7, we can easily write the following expression:

$$\alpha(x_1, T) = \frac{a_{\rho 1}(x_1)}{a_{\rho 0}(x_1) + a_{\rho 1}(x_1) \times T} \tag{8}$$

Using Eq. 8, it is interesting to calculate values of the isobaric thermal expansion (α) from the Table 2 data at given temperature and alloy composition or to predict and estimate its values for other temperatures and/or compositions using interpolation and extrapolation methods by modeling or scanning the plots of ($a_{\rho 0}$ and $a_{\rho 1}$) versus temperature (Figs. 4 and 5).

Fig. 4 shows a globally decrease of the parameter ($a_{\rho 0}$) with the molar fraction of tin (x_1) and spectacular plateau about 9.107 g·cm^{-3} in the composition domain between 0.1 and 0.45. Due to the atomic liquid structure and thermo-mechanical properties conflict, this phenomenon can be interpreted as being the establishment of equilibrium of a certain atomic structure during the introduction of tin into silver from 10% to 45 %. In addition, the mechanical behavior in the liquid state is intermediate between the behavior of the Hooke solid and that of the Newtonian liquid thus defining viscoelasticity. Moreover, in this special range of compositions, the mean free path during the atomic collisions

Table 2
Parameters values of Eqs. (5) and (6), and specific temperature (T_ρ) for the {Sn (1) + Ag (2)} systems vs. the molar fraction (x_1) of Sn through the interval of temperature (623.15 to 1223.15) K.

$x_1 = x_{Sn}$	$a_{\rho 0} = \rho_0$	$a_{\rho 1} = -\alpha\cdot\rho$	R	$T_\rho \times 10^{-3}$
-	g.cm^{-3}	mg.K^{-1}.cm^{-3}	-	K
0.000	10.195	-0.72778	0.99987	32.358
0.0686	9.2253	-0.34071	0.99891	27.077
0.1000	9.1180	-0.36032	0.99927	25.305
0.1500	9.1095	-0.45399	0.99972	20.065
0.2500	9.1095	-0.59426	0.99988	15.329
0.3000	9.0988	-0.67421	0.99986	13.495
0.3529	9.0688	-0.85273	0.99645	10.635
0.4000	9.0983	-1.1162	0.99932	8.1511
0.4761	9.0299	-1.3739	0.99983	6.5725
0.5000	8.9385	-1.3563	0.99991	6.5904
0.6000	8.3189	-0.97761	0.99973	8.5094
0.7000	7.7677	-0.63672	0.99981	12.200
0.7500	7.6317	-0.58569	0.99981	13.030
0.8200	7.4801	-0.54244	0.99947	13.790
0.8780	7.3822	-0.53216	0.99961	13.872
0.9000	7.3526	-0.53744	0.99974	13.681
0.9620	7.3098	-0.59972	1	12.189
1.000	7.3101	-0.61993	1	11.792

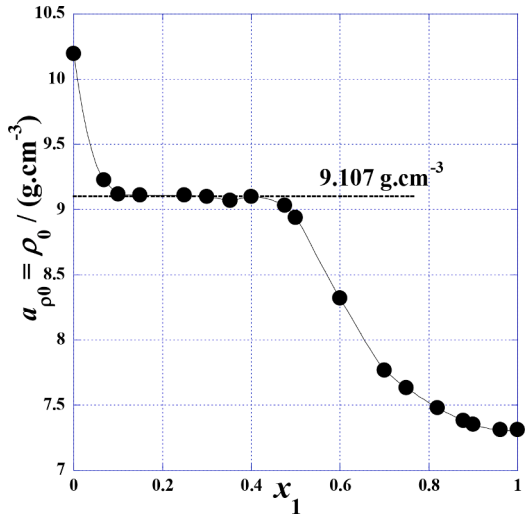

Fig. 4. Limiting density (ρ_0) for the {Sn (1) + Ag (2)} systems *vs.* the molar fraction (x_1) of Sn through the interval of temperature (623.15 to 1223.15) K.

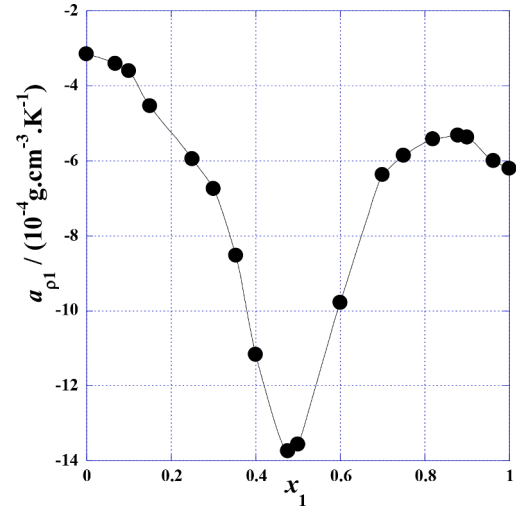

Fig. 5. Parameter ($a_{\rho 1}$) of Eq. 5, for the {Sn (1) + Ag (2)} systems *vs.* the molar fraction (x_1) of Sn through the interval of temperature (623.15 to 1223.15) K.

remains practically constant during the atomic collisions to maintain then the constancy of density depending on the parameters other than the temperature. Fig. 5 exhibits a local minimum at 0.45 of molar composition globally for the parameter ($a_{\rho 1}$) with the molar fraction of tin (x_1) showing that the effect of the variation in composition outweighs the effect of temperature in the phenomenon of liquid alloy expansion.

By similarity of Fig. 3, we have also plotted in Fig. 6 the ratio ($\rho_0/a_{\rho 1}$) which is equivalent to a specific temperature (T_ρ) in relationship to the thermal agitation in connection to the expansions phenomena and the mean free path during the atomic collisions in liquid state [11–24]. The value of this specific temperature (T_ρ) is an interesting criterion of the intensity of the interatomic forces inside the liquid far away from the free surface of liquid binary alloy due to thermal agitation.

However, to find more physical significance to the temperature parameters ($a_{\rho 0}$ and $a_{\rho 1}$), we have collected from literature some density information on the Sn-Ag alloys [5]. We conclude that the (ρ_0)-parameter is very close to the density of the same material is solid state at room temperature (Table 3). We can conclude that the knowledge of the density of an alloy at solid state can lead us to estimate in good approximation the value the ($a_{\rho 0}$)-parameter related to the density-temperature dependence of the same alloy composition at liquid

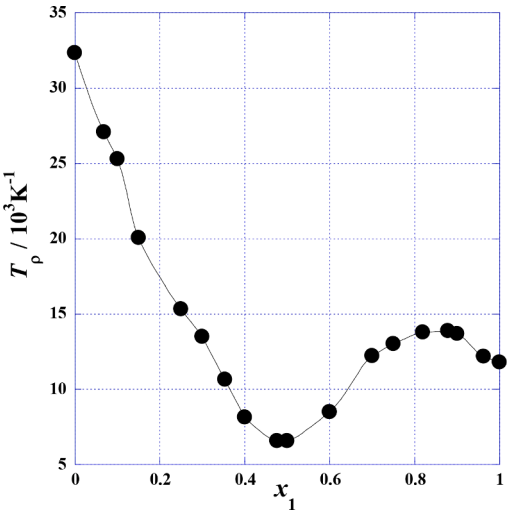

Fig. 6. Specific temperature (T_ρ) for the {Sn (1) + Ag (2)} systems *vs.* the mole fraction (x_1) of Sn through the interval of temperature (623.15 to 1223.15) K.

Table 3
Comparison between the limiting density (ρ_0) and the density of some similar system in solid state.

x_1	Density / g.cm^{-3}		$a_{\rho 0} = \rho_0$
	Liquid at melting point	Solid at room temperature	g.cm^{-3}
0.0 (Ag)	9.346 [40]	10.490 [41]	10.465 [40]
1.0 (Sn)	6.990 [42]	7.1761 [43]	7.3090 [42]
0.96 (w/w)	-	7.3900	7.3098

state.

The molar volume (V_m) values, depicted in Fig. S6 and presented in Table S4 are calculated using the following equation:

$$V_m(x_1, T, P) = \frac{x_1 M_1 + (1 - x_1) M_2}{\rho(x_1, T, P)} \tag{9}$$

Where M_1 and M_2 are the molar mass of the pure constituent of Sn and Ag respectively. Regarding the Eqs. 7, 8 and 9 we can rewrite the isobaric thermal expansion (α) and the molar volume (V_m) as follows:

$$\alpha(x_1, T) = \frac{1}{V_m(x_1, T)} \left(\frac{\partial V_m(x_1, T)}{\partial T} \right)_P \tag{10}$$

$$V_m = \frac{x_1 M_1 + (1 - x_1) M_2}{a_{\rho 0}(x_1) + a_{\rho 1}(x_1) \times T} \tag{11}$$

Using Eqs. 8, 9 and 11, it is interesting to calculate values of the isobaric thermal expansion (α) and the molar volume (V_m) from the Table 2 data at given temperature and alloy composition or to predict and estimate its values for other untreated temperatures and/or compositions using interpolation and extrapolation methods by modeling or scanning the plots of ($a_{\rho 0}$ and $a_{\rho 1}$) versus temperature Figs. 4 and 5) for eventual novel engineering materials. Furthermore, estimation of the isobaric thermal expansion (α) and the molar volume (V_m) values are necessary for thermodynamics investigations, thermophysical and calorithmetic studies (Eqs. 12, 13 and (14) or for well as for generalization to multi-constituent alloys requiring knowing of the data of the pure constituents and their binary alloys, etc.

$$\left(\frac{\partial V(x_1, T)}{\partial T} \right)_P = - \left(\frac{\partial S(x_1, T)}{\partial P} \right)_T \tag{12}$$

$$\left(\frac{\partial C_P(x_1)}{\partial V}\right)_{T,P} = -\left(\frac{\partial^2 H(x_1)}{\partial V \partial P}\right)_{T,P} \quad (13)$$

$$CP = CP0 + \alpha 0 \times Vm \quad (14)$$

Where Cp is the isobaric heat capacity at temperature T.

2.3. Dynamic viscosity with composition

Until now, a large part of the material has been treated in the liquid status, for example by casting or brazing processes. Thereby, the properties of the liquid substance have a strong influence on the properties and quality of the final material. Thus, for reasons of materials and process optimization, knowledge of the dynamic viscosity of a material is important.

From a physical point of view, the properties such as dynamics, viscosity, diffusion, and electrical resistivity are highly sensitive to structural changes with respect to temperature as well as sample composition. In a number of studies, [44,45] some conclusions have been initiated for the atomic structure via viscosity measurements. Thus, in addition to the technological aspect mentioned, the determination of the dynamic viscosity of liquid alloys will contribute to the considerate of the interaction flanked by composition and physical properties.

In order to clarify the nature of the maximum curved viscosity we can use one model among many ones to calculate the dynamic viscosities of binary alloys from those of the constituents proposed in the literature [46–49].

Several models have been presented in literature [50] to express the variation of dynamic viscosity of binary fluid mixtures with molar composition. All these models are practically based on the deviation of the viscosity ($\Delta\eta$) to the linearity expressed as follows:

$$\Delta\eta = \eta - (x_1\eta_1 + x_2\eta_2) \quad (15)$$

Where, η_1, η_2 and η represent the shear viscosity of pure constituents (1) and (2) and of the mixture, respectively.

Nevertheless, the deviation to the linearity (Eq. 15) doesn't generally reflect the real deviation to the ideality for the viscosity and several physicochemical especially the non-thermodynamic state function, like surface tension (σ), friccohesity (φ_h), refractive index (n), density (ρ), molar isobaric heat (C_{pm}), sound speed (c), isobaric thermal expansivity (α), dipolar momentum (μ), isentropic compressibility (κ_s) and dielectric constant (ε) [24–26].

In the present work, we will be interested in the Grunberg-Nissan model [51], which represents the best the deviation to ideality (Eq. 16) due to the logarithm form of dynamic viscosity (Fig. S7).

$$ln\eta = x_1 \cdot ln\eta_1 + x_2 ln\eta_2 + x_1 \cdot x_2 \cdot d_T \quad (16)$$

Where d_T is an interaction parameter depending only on the temperature and the nature of the binary mixture, the indexes 1 and 2 correspond to the pure constituents Sn(1) and Ag(2), respectively.

Table 4 and Fig. 7 present the variation of the Grunberg-Nissan interaction parameter with temperature showing that the amplitude of interaction diminishes in the thigh temperature region. The negativity of this parameter indicates the weak character of interatomic interaction into the binary Sn-Ag alloy. In addition, Grunberg-Nissan found that the interaction parameter (d_T) is negative for systems showing a positive deviation from Raoult's law and it's in relationship with the constant b in the simplified Margules equation [51–53].

The peculiar quasi-concordance of the Grunberg-Nissan interaction parameter (d_T) values with the opposite of the logarithm of viscosity of the binary Sn-Ag alloy ($-\ln\eta_T$) at the composition (x_1=0.0686) inspires us to examine the variation, with temperature (T), of (d_T) as well as ($\ln\eta_1$) and ($\ln\eta_2$) conforming to the Andrade law (Eq. 17).

$$\ln\eta i = Ai + Bi/T \quad (17)$$

where (i) designates (1) for Sn and (2) for Ag.

Indeed, Figs. S8 and S9 show practically a perfect linearity with the reciprocal absolute temperature ($1/T$) except a very slight deviation of the variation of (d_T) confirmed by the correlation R in Table 5 which presents the Andrade coefficients A_i and B_i.

However, our curiosity to uncover the mathematical trend of this feeble discrepancy to the linearity of the Grunberg-Nissan interaction parameter (d_T), inspired us to think about the linearization of the hyperbolic dependence with temperature and to plot the reciprocal values

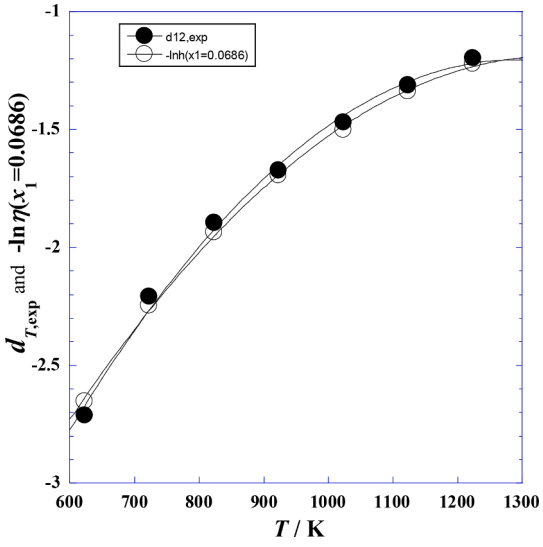

Fig. 7. The opposite of logarithm of viscosity of the alloy mixture (x_1=0.0686) and the experimental Grunberg-Nissan ($d_{T,exp}$) for the {Sn (1) + Ag (2)} systems *vs.* the temperature (T) of Sn through the interval of temperature (623.15 to 1223.15) K.

Table 4
Comparison between the experimental Grunberg-Nissan interaction parameter ($d_{T,exp}$) and those calculated ($d_{T,cal1}$) with Andrade Eq. 17; ($d_{T,cal2}$) with our suggested model Eq. 18.

T/K	$d_{T,exp}$	SE × 10^{-2}	$\sigma \times 10^{-2}$ [a]	$-\ln\eta_T(x_1$=0.0686)	$d_{T,cal1}$	$d_{T,cal2}$
623.15	-2.7119	14.287	7.6808	2.6539	-2.6515	-2.6990
723.15	-2.2104	10.736	5.9680	2.2460	-2.2458	-2.2311
823.15	-1.8947	7.7249	4.5157	1.9373	-1.9387	-1.9015
923.15	-1.6729	5.1382	3.2682	1.6956	-1.6981	-1.6567
1023.2	-1.4707	3.6885	2.5690	1.5019	-1.5044	-1.4677
1123.2	-1.3111	3.7828	2.6145	1.3403	-1.3453	-1.3174
1223.2	-1.1964	3.8458	2.6448	1.2212	-1.2123	-1.1951
			σ [b]	0.034298	0.035805	0.012613

[a] Standard deviation related to the difference between calculated and experimental values of the logarithm of viscosity expressed by the Grunberg-Nissan model (Eq. 16).
[b] Standard deviation related to the difference between calculated and experimental values of the logarithm of viscosity expressed by the Andrade model (Eq. 17).

Table 5
Optimal Andrade coefficients A_i and B_i values (Eq. 17) calculated from the logarithm of viscosity in mPa.s in Eq. 16.

	A_i -	B_i K	R -
$\ln\eta_T(x_1=1)$ of pure Sn	–0.69736	+650.55	0.99999
$\ln\eta_T(x_1=0)$ of pure Ag	–0.51621	+2303.1	0.99999
$\ln\eta_T(x_1=0.0686)$	–0.28233	+1828.2	0.99996
d_T	+0.38809	–1905.0	0.99859

$(1/d_T)$ with temperature (Fig. 8), discovering then a quasi-perfect linearity and leading us to express the dependence on temperature with two coefficients (T_0 and d_0) as follows:

$$d_T = \frac{T_0 d_0}{T - T_0} \tag{18}$$

Where T_0 = 145.70 K and d_0 = –8.8404 are independent of temperature. We note that the least mean square indicates that the correlation coefficient R is greater for Eq. 18 (0.99978) than for Eq. 17 (0.99859) which justifies the feeble discrepancy compared to the linearity, which is also confirmed by the low value of standard deviation in Table 4.

Though the Expression of Eq. 18 is well representative of the variation of the Grunberg-Nissan interaction parameter (d_T) with temperature, this parameter depends only on temperature (T), gives only a global information on the binary Sn-Ag alloy but lacks to offer precise value at given composition (x_1). So, some researchers expand the concept of Grunberg-Nissan by substituting the (d_T) which depends only on temperature by an equivalent one ($G_{12,T}$) which depends on both the temperature and the molar composition (x_1). ($G_{12,T}$) is determined by calculating the experimental value of (d_T) at each temperature and composition using the following equation,

$$G_{12,T}(x_1) = d_{T,exp}(x_1) = \frac{ln\eta - (x_1 \cdot ln\eta_1 + x_2 ln\eta_2)}{x_1 \cdot x_2} \tag{19}$$

The extended new Grunberg-Nissan model becomes expressed as follows.

$$ln\eta = x_1 \cdot ln\eta_1 + x_2 ln\eta_2 + x_1 \cdot x_2 \cdot G_{12}(x_1, T) \tag{20}$$

Table 6 gives values of the new Grunberg-Nissan interaction parameter $G_{12,T}(x_1)$ and Fig. 9 shows the variation of this parameter with molar fraction (x_1) of Sn compositions. We can see that the

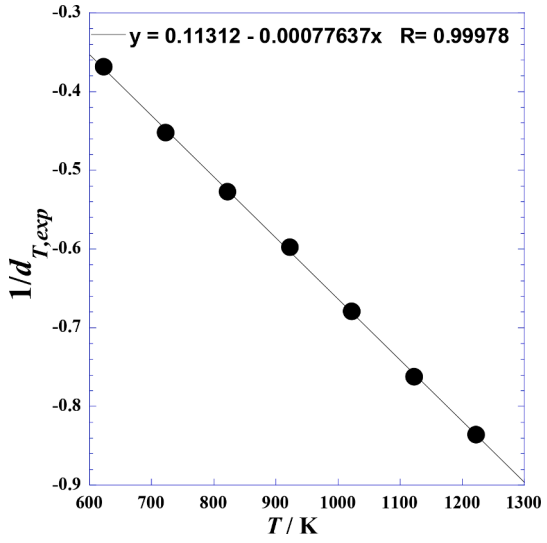

Fig. 8. The reciprocal of the experimental Grunberg-Nissan ($1/d_{T,exp}$) for the {Sn (1) + Ag (2)} systems *vs.* the temperature (T) of Sn through the interval of temperature (623.15 to 1223.15) K.

experimental Grunberg-Nissan interaction parameter $G_{12,T}(x_1)$ versus temperature and composition can give retailed information to eventual atomic interactions, changes of structure and prediction of the isobaric binary diagram through the peculiar compositions limiting some regions with different behaviors [25,26,51–53] and which is more revealed or pointed out in Fig. S10 by the plot of the reciprocal of the Grunberg-Nissan interaction parameter $1/G_{12,T}(x_1)$.

In addition, the reduced Redlich-Kister excess function $Q_{Y,T}(x_1)$ has been introduced in previous work [24] for revealing different types of interactions (Eq. 21) especially at high and low molar compositions.

$$Q_{Y,\exp,T}(x_1) = \frac{Y^E}{x_1(1-x_1)} \tag{21}$$

Comparison between the Eqs. 19 and 21, we can see that the new Grunberg-Nissan interaction parameter $G_{12,T}(x_1)$ is none other than the reduced Redlich-Kister property $Q_{Y,T}(x_1)$ related to the logarithm of dynamic viscosity (Y=lnη) of the binary Sn-Ag liquid alloy. We can also add that the comparison between the Eqs. 16 and 20 shows that the parameter (d_T) of Table 4 can be determined by the average value of the function $G_{12,T}(x_1)$ taken from the Table 6 at given temperature (T) and which is defined by the integral expressed as follows.

$$d_T = \int_0^1 G_{12}(x_1, T) dx_1 \tag{21}$$

The expression of the function $G_{12,T}(x_1)$ must be adequately chosen from the curves' trend in Fig. 9 by non linear regression and if necessary using a piecewise function for two intervals.

3. Viscosity Arrhenius behavior

Otherwise, it is observed that the dynamic viscosity-temperature dependence can be generally obtained using the Arrhenius-type equation as follows:

$$\eta = A_s . e^{\frac{Ea}{RT}} \tag{22}$$

Where *Ea, R* and *As* are, the activation energy, the ideal gas constant and the pre-exponential factor of the Arrhenius-type equation for the studied system, respectively. Under the natural logarithmic form, we can be also rewrite the Eq (22) as follows:

$$\ln\eta = \ln A_s + \frac{E_a}{R}\left(\frac{1}{T}\right) \tag{23}$$

Fig. S11 shows clearly that the natural logarithm of dynamic viscosity ln(η) for which we plotted the dependence versus the inverse of absolute temperature ($1/T$) for Sn (1) + Ag (2) alloy systems in the whole domain of molar composition(x_1)is practically linear for absolute temperature over the studied absolute temperature domain (623.15 to 1223.15) K with a mean correlation coefficient R(mean) = 0.99977, and the Arrhenius parameters *Ea* and *As* are thus independent of absolute temperature. Using both least-squares fitting methods and graphics, *ln* (*As*) is the *y*-intercept and *Ea*/*R* is the slope of the straight line (Table 7) either for their corresponding systems ($x_1 \neq 0$) or for the pure constituents (i.e. at $x_1 = 0$ or $x_1 = 1$). Figs. 11 and 12 show the variation of the main Arrhenius parameters *Ea* and ln*As vs.* mole fraction x_1 of tin. We see that the activation energy (*Ea*) decreases exponentially with (x_1) while *ln*(*As*) increases starting from the value of the pure silver to reach a short plateau centered by (x_1=0.2), after that, it decreases to reach a second short plateau centered by (x_1=0.5) and decreases to the value of the pure tin. Given that *ln*(*As*) is a disorder factor since it is in relationship with the entropy [27–30], its variation can give some indication about the equilibrium phase diagram for silver and tin.

$$T_A = -\frac{E_a}{R \cdot lnAs} \tag{24}$$

Table 6
Experimental Grunberg–Nissan parameter $G_{12,T}(x_1)$ (Eq. 19) for Sn (1) +Ag (2) mixtures against molar fraction x_1 in Sn through the interval of temperature (623.15 to 1223.15) K.

Molar fraction	Grunberg- Nissan interaction parameter $G_{12,T}(x_1)$						
$x_1 = x_{Sn}$	623.15K	723.15K	823.15K	923.15K	1023.15K	1123.15K	1223.15K
0.000[a]	-7.7519	-5.8140	-4.2194	-3.2680	-2.3866	-1.7938	-1.3981
0.0686	-5.1866	-3.9661	-3.0359	-2.3067	-1.7230	-1.2687	-0.99624
0.1000	-4.5072	-3.4904	-2.7277	-2.0455	-1.5876	-1.0518	-0.85919
0.1500	-3.6726	-2.9482	-2.3881	-1.7020	-1.4056	-0.82380	-0.69827
0.2500	-2.9235	-2.3473	-1.7898	-1.3900	-1.1659	-0.77568	-0.66998
0.3000	-2.8162	-2.1941	-1.7480	-1.3991	-1.1213	-0.89051	-0.77050
0.3529	-2.7223	-2.2051	-1.8269	-1.6220	-1.3099	-1.1372	-0.96648
0.4000	-2.8346	-2.2840	-1.9240	-1.7169	-1.4665	-1.2942	-1.1397
0.4761	-2.9231	-2.3457	-2.0508	-1.8201	-1.6365	-1.4839	-1.3546
0.5000	-2.8375	-2.3100	-1.9993	-1.7743	-1.5845	-1.4394	-1.3121
0.6000	-2.5003	-2.1025	-1.7995	-1.5626	-1.3735	-1.2168	-1.1346
0.7000	-2.2228	-1.8627	-1.6217	-1.4551	-1.2720	-1.1027	-1.0345
0.7500	-2.0909	-1.7622	-1.5506	-1.4058	-1.2318	-1.0554	-0.99581
0.8200	-1.9449	-1.6212	-1.4495	-1.3051	-1.1760	-0.99485	-0.94700
0.8780	-1.8678	-1.5250	-1.3716	-1.2347	-1.1326	-0.95442	-0.91110
0.9000	-1.8474	-1.5128	-1.3426	-1.2138	-1.1131	-0.94537	-0.90016
0.9620	-1.7601	-1.4463	-1.2638	-1.1673	-1.0600	-0.91937	-0.88042
1.000[b]	-1.7298	-1.4222	-1.2367	-1.1505	-1.0470	-0.91140	-0.87512

[a] Extrapolated values obtained by non linear regression of $G_{12,T}(x_1)$ with polynomial of four degree *vs.*x_1 taking the obtained first polynomial coefficient (at x_1 =0) for the interval [0,0.5] in x_1.
[b] Extrapolated values obtained by non linear regression of $G_{12,T}(x_2)$ with polynomial of four degree *vs.*x_1 taking the obtained first polynomial coefficient (at x_2 =0) for the interval [0,0.5] in x_2.

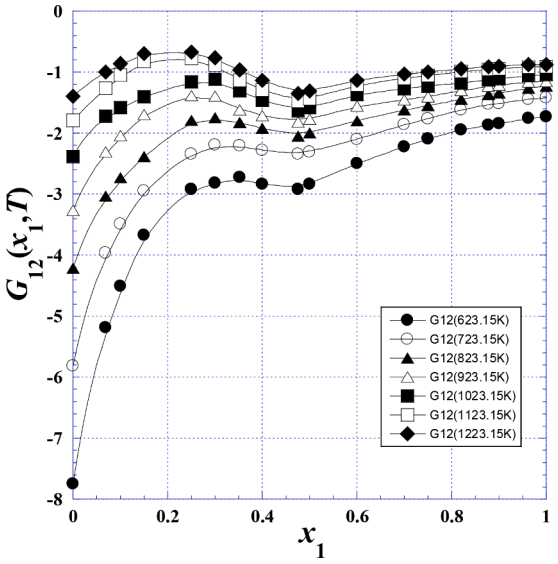

Fig. 9. The experimental Grunberg–Nissan parameter $G_{12,T}(x_1)$ (Eq. 19) for Sn (1) +Ag (2) mixtures against molar fraction x_1 in Sn at temperatures from (623.15 to 1223.15) K.

$$T^* = \frac{E_a}{R} \tag{25}$$

However, the Arrhenius temperature (T_A) as a third dependent parameter (Eq. 24) can be considered as an interesting criterion for discussion. For this reason, we have plotted its variation with the molar fraction (Fig. S12) for which the exponential decrease is affected by the variation of $Ea(x_1)$ in Fig. 10 and not by that of $\ln As(x_1)$ in Fig. 11 because the variation interval of $\ln As$ is not large (about –7.390±3%). To well model this variation, we have plotted in Fig. S13 the two Arrhenius parameters product with one parameter (Ea), which led us to discover an interesting linear dependence (Fig. 12) of the reciprocal of Arrhenius temperature ($1/T_A$) expressed as follows:

$$\frac{1}{T_A} = \frac{x_1}{T_{A1}} + \frac{x_2}{T_{A2}} \tag{26}$$

Where (T_{A1}) and (T_{A2}) correspond to the Arrhenius temperatures of the pure Ag and Sn, respectively. We can conclude that it can be an interesting tool to predict (T_A) for any composition of the binary tin-silver alloy.

In addition, we can investigate another interesting parameter [27–30] such as the current Arrhenius temperature (T_{Ac}), expressed by the Eq. 27. We observe two singularities at the two molar fractions 0.17 and 0.52 which can be probably in connection with the equilibrium phase diagram for silver and tin (Fig. 13).

$$T_{Ac} = \frac{\partial E_a}{\partial(-RlnAs)} \tag{27}$$

Finally, inspiring from prediction of the boiling temperature through the viscosity activation energy (Ea) for classical solvents [27–30,50,54,55], we can calibrate previous empirical model for specific parameters for our studied binary {Sn (1) + Ag (2)} alloy and suggest the following expression:

$$T_b = \frac{E_a}{\alpha + \beta E_a} \tag{28}$$

Where $\alpha = (-0.4738 \pm 0.0013))JK^{-1}mol^{-1}$ and $\beta = (4.354 \pm 0.021) \times 10^{-4}K^{-1}$

We can conclude that this empirical expression gives excellent values of the boiling temperature of the pure Ag and Sn, and we wish that the application of this model for a given binary tin-silver alloy (Table 4) can give reliable estimation of the corresponding boiling point useful for solder.

4. Activation of viscous flow parameters

Adopting the concept of the absolute reaction rate theory of Ali *et al.* [56] and Eyring *et al.* [57] for the binary alloy fluid phase, the free Gibbs energy (ΔG^*) of activation of viscous flow (Table S5, Fig. S14) is expressed as follows:

$$\Delta G^*(x_1,T,P) = RT \cdot ln\left(\frac{\eta(x_1,T,P)\cdot V(x_1,T,P)}{hN_A}\right) \tag{29}$$

where R, η, h, N_A and V are the ideal gas constant, dynamic viscosity of binary alloy system, Plank's constant, Avogadro's number and molar

Table 7
Activation energy of Arrhenius *Ea* / (kJ·mol^{-1}), Arrhenius pre-exponential factor *As* / (mPa·s), the entropic factor of Arrhenius –*R*·ln(*As*/Pa·s) / (J·K^{-1}·mol^{-1}), Arrhenius temperature T_A (Eq. 24), activation temperature T^* (Eq. 25) and estimated boiling temperature $T_{b,est}$ (Eq. 28) for {Sn (1) + Ag (2)} systems *vs.* the molar fraction (x_1) of Sn through the interval of temperature (623.15 to 1223.15) K.

$x_1 = x_{Sn}$	ln(*As*/Pa.s)	T^*	*Ea*	-*R*.ln*As*	*As*	T_A	$T_{b,est}$
-	-	K	kJ.mol^{-1}	J.K^{-1}.mol^{-1}	mPa.s	K	K
0.000	-7.4242	2303.2	19.150	61.728	0.59666	310.23	2435.1
0.0686	-7.1902	1828.3	15.201	59.783	0.75391	254.27	2473.8
0.1000	-7.1503	1700.1	14.135	59.451	0.78461	237.77	2488.3
0.1500	-7.1321	1556.9	12.945	59.300	0.79901	218.29	2507.5
0.2500	-7.1306	1331.2	11.068	59.287	0.80025	186.69	2547.2
0.3000	-7.1773	1254.7	10.432	59.675	0.76371	174.82	2564.2
0.3529	-7.2986	1215.8	10.109	60.684	0.67650	166.58	2573.8
0.4000	-7.3538	1135.6	9.4419	61.143	0.64017	154.42	2595.9
0.4761	-7.4456	1033.5	8.5930	61.906	0.58398	138.81	2629.8
0.5000	-7.4471	1001.8	8.3294	61.919	0.58312	134.52	2641.9
0.6000	-7.4514	888.20	7.3849	61.954	0.58064	119.20	2693.7
0.7000	-7.5057	828.15	6.8856	62.405	0.54997	110.34	2727.9
0.7500	-7.5327	802.40	6.6715	62.630	0.53531	106.52	2744.4
0.8200	-7.5590	761.55	6.3319	62.849	0.52140	100.75	2773.4
0.8780	-7.5737	723.40	6.0147	62.971	0.51379	95.515	2804.1
0.9000	-7.5811	710.13	5.9043	63.032	0.51002	93.672	2815.7
0.9620	-7.5950	672.39	5.5906	63.148	0.50297	88.531	2851.9
1.000	-7.6052	650.59	5.4093	63.233	0.49787	85.546	2875.2

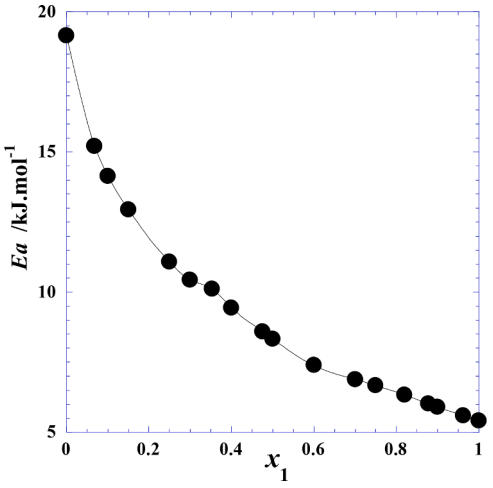

Fig. 10. The viscosity activation energy (*Ea*) of Eq. 23 for the {Sn (1) + Ag (2)} systems *vs.* the molar fraction (x_1) of Sn through the interval of temperature (623.15 to 1223.15) K.

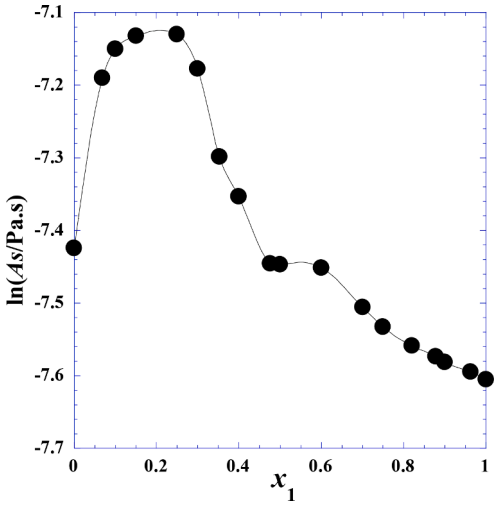

Fig. 11. The logarithm of pre-exponential factor ln(*As*) of Eq. 23 for the {Sn (1) + Ag (2)} systems *vs.* the molar fraction (x_1) of Sn through the interval of temperature (623.15 to 1223.15) K.

volume of binary alloy system (Eq. 9), at molar fraction (x_1), absolute temperature *T* and pressure *P*, respectively, and:

$$\Delta G^* = \Delta H^* - T\Delta S^* \tag{30}$$

Where ΔH^* and ΔS^* are the entropy and the enthalpy of activation of viscous flow. By assuming that the two parameters of activation of viscous flow ΔS^* and ΔH^* [56,57] are practically independent of the absolute temperature. Then, in Fig. S15 the ratio ($\Delta G^*/T$) against $1/T$ is represented in the studied domain of absolute temperature from 623.15 K to 1223.15 K for the binary alloy of Sn(1)+Ag(2) systems at some representative molar fractions of Sn, the result clearly shows a positive slope of linear behavior with. Using both, graphical method and least-square fit, the *y*-intercept is equal to ($-\Delta S^*$) and the slope is equal to ΔH^*. Values of the entropy ΔS^* of activation of viscous flow and the enthalpy ΔH^* are given in Table 8, and plotted in Figs. 14 and 15 with molar fraction of Sn. We observe interesting similar behaviors between the two parameters of activation of viscous flow and the two viscosity Arrhenius parameters (ΔH^* and *Ea*) and (ΔS^* and –*R*·ln*As*).

We can add that the increment between each couple of variables shown in (Figs. 14 and 15) leads us to consider that the activation energy (*Ea*) and the entropic factor (–*R*·ln*As*) can be approximately considered as a thermodynamic state function.

In consideration of some thermodynamic Maxwell relations and the Eqs. 7, 9, 10, 12, 23, 29 and 30, we can see that the isobaric thermal expansion coefficient (α) of the binary alloy system (Eqs. 7 or 10) is related to the enthalpy increment which is expressed by (Eq. 31). Furthermore, the entropy increment δS^* is equal to the difference between the two activation energies related to the kinematic and dynamic viscosity respectively (Eq. 32).

$$Ea - \Delta H^* = R\alpha T^2 \tag{31}$$

$$\delta S^* = R\cdot\left[\ln\left(\frac{V(x_1,T,P)}{hN_A}\right) + \alpha\cdot T\right] \tag{32}$$

Finally to contribute for researchers in modeling and prediction, we have plotted in Fig. S16 the two thermodynamic parameters product ($-\Delta H^*\Delta S^*$) against one parameter (ΔH^*), which led us to discover an interesting quasi-linear dependence (Fig. S16) for enthalpy values less than (12kJ·mol^{-1}) i.e. in the tin rich region (Table 8). Nevertheless, we can describe the whole compositions' region with a three-degree

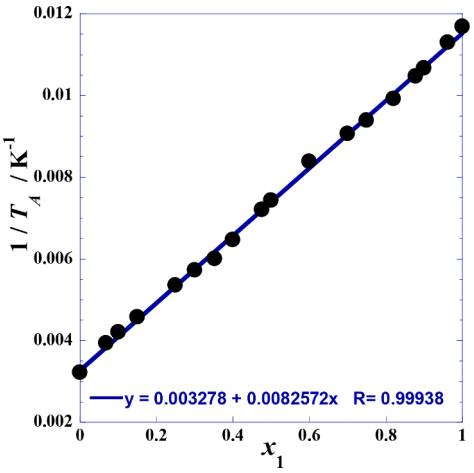

Fig. 12. The reciprocal of the Arrhenius temperature ($1/T_A$) for the {Sn (1) + Ag (2)} systems *vs*. the molar fraction (x_1) of Sn through the interval of temperature (623.15 to 1223.15) K.

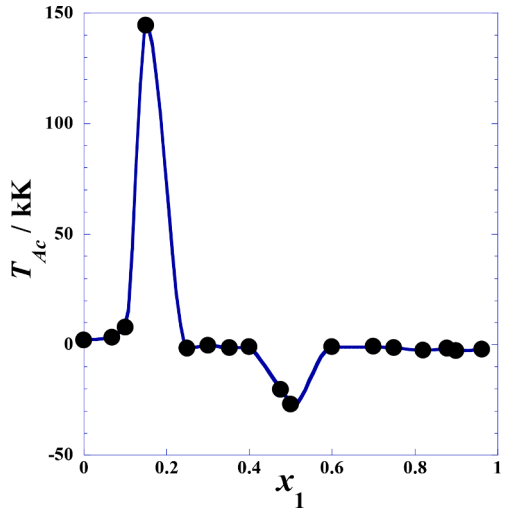

Fig. 13. The current Arrhenius temperature (T_{Ac}) for the {Sn (1) + Ag (2)} systems *vs*. the molar fraction (x_1) of Sn through the interval of temperature (623.15 to 1223.15) K.

Table 8
Thermodynamic parameters of the {Sn (1) + Ag (2)} systems *vs*. the molar fraction (x_1) of Sn through the interval of temperature (623.15 to 1223.15) K.

$x_1 = x_{Sn}$	ΔS^* J.K^{-1}.mol^{-1}	ΔH^* kJ.mol^{-1}	$x_1 = x_{Sn}$	ΔS^* J.K^{-1}.mol^{-1}	ΔH^* kJ.mol^{-1}
0.000	-24.071	18.672	0.5000	-26.782	7.2288
0.0686	-26.351	14.964	0.6000	-26.807	6.5595
0.1000	-26.848	13.880	0.7000	-26.393	6.3315
0.1500	-27.212	12.618	0.7500	-26.267	6.1558
0.2500	-27.553	10.634	0.8200	-26.200	5.8466
0.3000	-27.361	9.9349	0.8780	-26.225	5.5318
0.3529	-26.764	9.4578	0.9000	-26.231	5.4140
0.4000	-26.809	8.5736	0.9620	-26.359	5.0358
0.4761	-26.697	7.4904	1.000	-26.349	4.8343

polynomial with an excellent agreement where the corresponding coefficients values are given in Fig. S16.

5. New concept of friccohesity in binary fluid alloys

Constitutionally the friccohesity [31–35,58–60] being an index of the

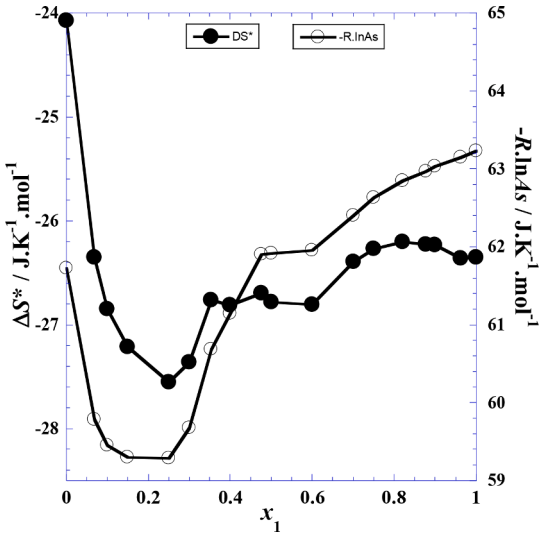

Fig. 14. The entropic factor ($-R{\cdot}\ln As$) of Eq. (23) and the entropy (ΔS^*) of activation of viscous flow of Eq. (30) for the {Sn (1) + Ag (2)} systems *vs*. the molar fraction (x_1) of Sn through the interval of temperature (623.15 to 1223.15) K.

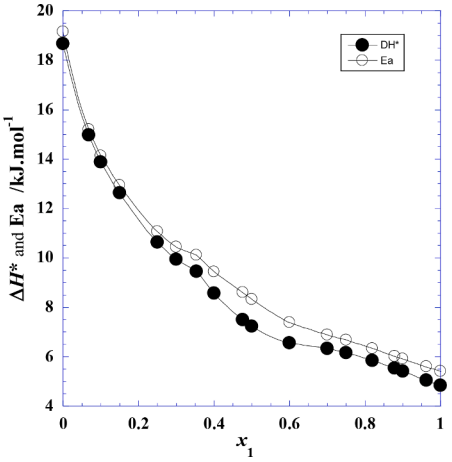

Fig. 15. The viscosity activation energy (*Ea*) of Eq. (23) and the enthalpy ΔH^* of activation of viscous flow of Eq. (30) for the {Sn (1) + Ag (2)} systems *vs*. the molar fraction (x_1) of Sn through the interval of temperature (623.15 to 1223.15) K

cohesive forces and the adhesive forces of fluids of the metallic binary alloy depicts an orientational mutually alignment of Sn + Ag together as per their electronic configurations Ag ($1s^2 2s^2 2p^6 3s^2 3p^6 4s^2 3d^{10} 4p^6 d^{10} 5s^1$) and Sn ($1s^2 2s^2 2p^6 3s^2 3p^6 4s^2 3d^{10} 4p^6 5s^2 4d^{10} 5p^2$) and also on increasing compositions of the Sn added to the Sn+Ag material. Fig. 16 infers a decreasing order of friccohesity with increasing composition of Sn metal with Sn-Ag material. However, the slope from 623.15 to 1223.15K is lowered and the friccohesity at the 1223.15K seems to decrease linearly following a first order decrease. These trends depict that the Sn seem to be strongly clustered with the Sn+Ag alloy where the Ag could act as a doping agent as per concept of the Schottky and Frenkel for doping mechanism. Since increasing population of the Sn might have been aligned around the Sn of the Sn+Ag alloy that increased the cohesive forces by lowering the friccohesity because the surface tension depicts the cohesive forces [31–35,58–60]. The energy of a particle or an electron in orbit of an atom is defined as.

$$\left(E + \frac{e^2}{r}\right)^2 \psi(x) = \nabla^2\psi(x) + m^2\psi(x) \quad (33)$$

Electron energy e, distance between them is r, electronic wave function ψ electronic cloud oscillatory area intensity, x location of electron, and m is mass. The friccohesity and activation energy are the languages of the quantum chemistry where the mono-dispersion of the homogenized metallic mixtures develop unique physicochemical properties. The x distance between the Sn atom which is added to the Sn+Ag is lowered so the potential energy is increased [31–35,58–60].

The friccohesity of {Sn(1)+Ag(2)} binary alloys *vs.* composition of Sn over temperature from 623.15 to 1223.15K decreases. It proves that the Sn has homogenized the alloy with slightly more orientation of added Sn towards the Sn of the alloy. A higher temperature decreases the friccohesity on increasing the Sn mole fractions but at 1223.15 K, it opts an almost first order decrease with lower negative slope compared to its values at 623.15K. This proves that the higher thermal energy seems to intensely pack these metallic atoms together against their oscillatory motions. Thus, the friccohesity indicates that the cohesive forces of the Sn+Ag vis-a-vis added Sn atoms seem to develop a strongly packed cluster with additionally stronger cohesion. Hence on increasing the Sn population the Ag could act as doping agent within the Sn+Ag nano-cluster because friccohesity predicts stronger cohesion potential or binding potential on the Lennard-Jones potential scale with a lowest compressibility [31–35,58–60].

Fundamentally the friccohesity plotted in Fig. 16 explores a remarkable information about arrangement of the Sn+Ag alloy material with increasing temperature where at higher temperature the electronic oscillations of the Sn and Ag atoms with increasing population of the Sn probably get needful kinetic energy to occupy the space. It enables the system to cohere more and more Sn atoms with the Sn of the alloy pushing the Ag as dormant making ally a useful semiconductor material, but higher thermal energy saturate the cohesion of the adding Sn to the alloy that produces a 1st order lower decrease in slope i.e., the lower friccohesity. In general, the lower friccohesity infers stronger cohesive forces and lower viscous forces and it generates a valuable friccohesity chemistry where the frictional forces get weakened [31–35,58–60].

5.1. Apparent friccohesity with composition

Due to the lack of real friccohesity data and which it is very close to the ratio viscosity (η) on surface tension (σ), we have seen to treat this ratio as an apparent friccohesity (φ_{ha}) in the present system of Ag-Sn binary alloy.

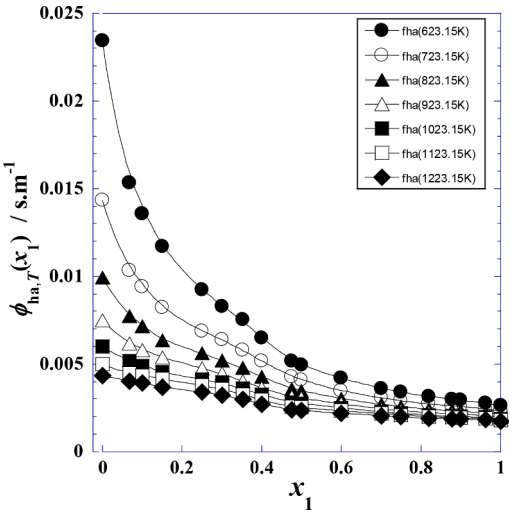

Fig. 16. The apparent friccohesityφ_{ha} (s·m^{-1}) of {Sn (1) + Ag (2)} systems vs. the molar fraction (x_1) of Snthrough the interval of temperature (623.15 to 1223.15) K.

$$\varphi_{ha} = \frac{\eta}{\sigma} \quad (34)$$

However, contrary to the viscosity the friccohesity being the dual force theory accurately explore a mechanism of the spatial arrangements of the alloy because the surface tension that is generated due to the cohesive forces illustrate the coagulation of the similar atoms.

Table S6 in Supplementary Materials presents results of the apparent friccohesity (φ_{ha}) at different composition and temperatures that explore the mechanism of the distribution of the additional Sn in the Sn+Ag alloy matrix. The friccohesity values decrease at higher temperature because the Sn gets associated with Sn of the alloy where the Ag seems to act a dopant. On increasing temperature, we see that the apparent friccohesity decreases exponentially from the pure silver to the pure tin (Fig. 16) that infers a stronger packing activity due to higher thermal energy. The higher kinetic energy at higher temperature generates stronger translational, rotational, vibrational, electronic motions, which orient and bring the metallic atoms closer to each other and hence the cohesive forces are increased which are responsible for lowering the friccohesity values. Thus, the apparent friccohesity decreases with temperature of Sn+Ag where the added Sn atoms reorient themselves around Sn of the alloy shifting Ag as dopant position. However, at 1223.15K such alignments get saturated, and decrease is lower compared to a decrease at 623.15K. Hence the 1223.15K shifts the arrangements to a non-compressible alloy.

Generally, the majority of models are practically based on the deviation of physicochemical properties (ΔY) to the linearity expressed as follows:

$$\Delta Y = Y - (x_1 Y_1 + x_2 Y_2 \quad (35)$$

Where, Y_1, Y_2 and Y represent the property of pure constituents (1) and (2) and of the mixture, respectively. Still the nature of the constituents matters a lot whenever they are mixed in specific stoichiometric ratios.

The concavity of all curvatures in Fig. 16 indicates that the apparent friccohesity deviation $\Delta\varphi_{ha}$ is negative (Fig. S17), showing that the interatomic interactions between unlike atoms Sn and Ag in alloy are weak, while the atomic interactions between the similar atoms like Sn and Sn are stronger.

Nevertheless, the experimental values of the apparent friccohesity deviation $\Delta\varphi_{ha}$ tend to zero in the two limits of compositions domain due to the molar fraction product ($x_1 \cdot x_2$) of the Redlich-Kister (RK) polynomial [24–28,61–65] in Eq. 36.

$$\Delta Y = x_1(1-x_1)\sum_{p=0}^{p=n} A_{p,T}(2x_1 - 1)^p \quad (36)$$

So, the RK polynomial can be initiated by the ratio between the experimental excess property (Y^E) and the molar fraction product ($x_1 \cdot x_2$). This (Q_Y)-Quotient is named the experimental reduced Redlich-Kister property $Q_{Y,\exp,T}(x_1)$ which is formulated as follows:

$$Q_{Y,\exp,T}(x_1) = \frac{\Delta Y}{x_1(1-x_1)} \quad (37)$$

As has been commented by Desnoyers and Perron [61], the excess thermodynamic functions of state have an advantage in elucidating the magnitude and sign of their non-ideality [62], but reduced R-K quantity $\Delta Y/x_1(1-x_1)$ give a widely deal superior handling on the source of the non-ideality.

Desnoyers and Perron add that the reduced R-K excess property is additional responsive than the direct excess one Y^E, to intermolecular interactions that occurs at low molar fractions [24–28,61–65]. In point of view of cohesion, the Fig. S18 shows that the introduction of Sn atoms in pure Ag is more difficult the reverse case.

However, our curiosity in modeling incites us to test the deviation to

the linearity of the reciprocal apparent friccohesity $\Delta\varphi_{ha}{}^{-1}$ using the Eq. 37 expressed as follows.

$$\left(\frac{1}{Y}\right)^{E} = \frac{1}{Y} - \left(\frac{x_1}{Y_1} + \frac{x_2}{Y_2}\right) \tag{38}$$

We discover that this excess property reveals some particular compositions (Fig. 17) interesting for the study of the isobaric binary diagram through the peculiar compositions limiting some regions with different behaviors where the interacting activities of each metal contribute to homogenized the formulations [25,26,51–53].

5.2. Apparent friccohesity with temperature

On the other hand, it is observed that the apparent friccohesity-temperature dependence obeys the Arrhenius-type equation as follows:

$$\varphi_{ha} = (\varnothing_v).e^{\frac{E\varphi}{RT}} \tag{39}$$

Where E_{φ}, R and Φ_v are, the activation energy, the ideal gas constant and the pre-exponential factor of the Arrhenius-type equation for the studied system, respectively (Fig. S19). Results are presented in Table 9 and depicted in Fig. 18.

5.3. Apparent friccohesity-viscosity correlation

Figs. 19 shows interesting linear correlation for each fixed temperature between the apparent friccohesity φ_{ha} ($s{\cdot}m^{-1}$) and the dynamic viscosity (η). We observe two linear dependences separated by a molar composition in connection with the isobaric binary diagram.

The Fig. 19 exceptional distinguishes a mechanism of the friccohesity considered as a dual force property and the viscosity as single forces theory. The friccohesity is calculated out of index of the cohesive and the adhesive forces while the viscosity is determined through the viscous or the adhesive forces. Therefore, the friccohesity *vs.* viscosity on increasing temperature from pure Sn and pure Ag develop the critical shift on increasing Sn mole fractions (Fig. 19). These shifts infer alignments of the added Sn whether these added Sn tends to align the Sn of the alloy or the cluster with the Ag. Since there is a decrease in friccohesity and viscosity both on increasing temperature and the shift noted at x_1=0.35, 0.33 and 0.31 at 623.15, 923.15, and 1223.15K respectively that infer Ag behaving as a dopant and Sn align around Sn of the alloy. Thus, the friccohesity data as sensor is of great significance to explore the role of the added atoms in the specified alloy mixture.

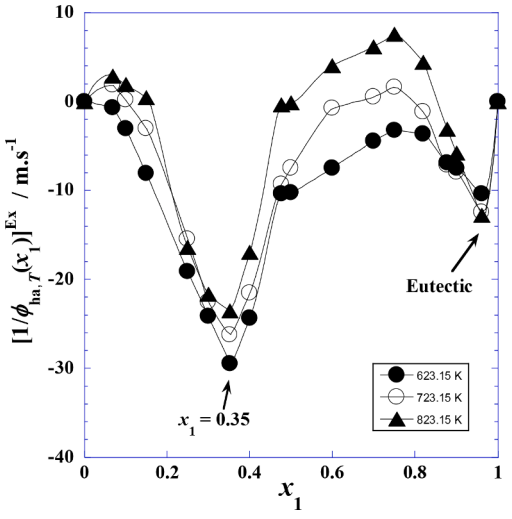

Fig. 17. Deviationof the reciprocal apparent friccohesity $\Delta\varphi_{ha}{}^{-1}$ ($m{\cdot}s^{-1}$) of {Sn (1) + Ag (2)} systems *vs.* the mole composition (x_1) of Sn through the interval of temperature (623.15 to 1223.15) K.

Table 9
Friccohesity activation energy E_{φ} / ($kJ{\cdot}mol^{-1}$) and Pre-exponential factor Φ_v / ($10^{-3}s{\cdot}\ m^{-1}$) for {Sn (1) + Ag (2)} systems vs. the molar fraction (x_1) of Sn through the interval of temperature (623.15 to 1223.15) K.

$x_1 = x_{Sn}$	$\ln(\Phi_v/s{\cdot}m^{-1})$ -	E_{φ} $kJ{\cdot}mol^{-1}$	Φ_v $ms{\cdot}m^{-1}$
0.000	-7.2147	17.875	0.73569
0.0686	-6.9271	14.186	0.98084
0.1000	-6.8588	13.198	1.0502
0.1500	-6.7997	12.078	1.1141
0.2500	-6.7089	10.446	1.2200
0.3000	-6.7087	9.9466	1.2202
0.3529	-6.7742	9.7570	1.1429
0.4000	-6.8230	9.2956	1.0885
0.4761	-6.8541	8.3090	1.0551
0.5000	-6.8344	7.9629	1.0761
0.6000	-6.7797	6.7362	1.1366
0.7000	-6.7830	5.9947	1.1329
0.7500	-6.7831	5.6503	1.1328
0.8200	-6.7825	5.2558	1.1334
0.8780	-6.7739	4.9581	1.1432
0.9000	-6.7706	4.8348	1.1470
0.9620	-6.7540	4.4739	1.1662
1.000	-6.7885	4.3184	1.1267

6. Double dependence on temperature and composition

In the previous sections, we have studied separately the dependence with temperature and the dependence with the molar composition. For engineering use and compilation, it's interesting to combine the found models to give common expressions to facilitate estimation and prediction of any property value at given temperature and composition of the binary alloy. So, the calculations of surface tension, density, and viscosity versus both the temperature and the molar fraction (x_1) of Sn are summarized in Tables 10, 11 and 12. Due to some curvature changes of some parameters abovementioned, we are forced to use high degree polynomials to minimize the discrepancy between calculated and experimental data.

7. Conclusion

The designing and development of ternary, quaternary and quinary alloys have received a great attentiveness particularly for lead-free solders which are widely applied in electronics. Experimental handlings of their physical and chemical properties are very sensitive and implicate specific and expensive devices. So, the investigations of binary alloy systems followed by theoretical generalization to alloys including more than three constituents find more easiness and can offer low costs. The mutual and chemical adhesion of the metallic constituents is an essential condition for developing the alloys and hence the friccohesity chemistry becomes the most desirable parameter for study by transforming their cohesive or the binding energies into the kinetic energy, which is urgently needed for their mutual adherences.

In the present work, the molar volume, surface tension, density, viscosity, friccohesity, and their derived properties of binary alloys Sn-Ag are implemented in the entire range of molar fraction at atmospheric pressure and at temperatures range (623–1123) K. These investigations were realized for the reason of bringing to light the effect of different types of interatomic interactions in binary alloys at liquid state by availing the variation of the physicochemical properties and its derived ones, especially the isobaric thermal expansion (α), the Grunberg-Nissan interaction parameter $G_{12,T}(x_1)$, the viscosity activation energy, the Arrhenius temperature, the thermodynamic Activation of viscous flow parameters and the new concept of friccohesity which is introduced at a first time for metal alloys. In this context, we affirm that the friccohesity data have acted as sensor and authentically defined the role of each constituent of the metallic alloys in case of Sn+Ag on increasing temperature. The friccohesity property being dual forces

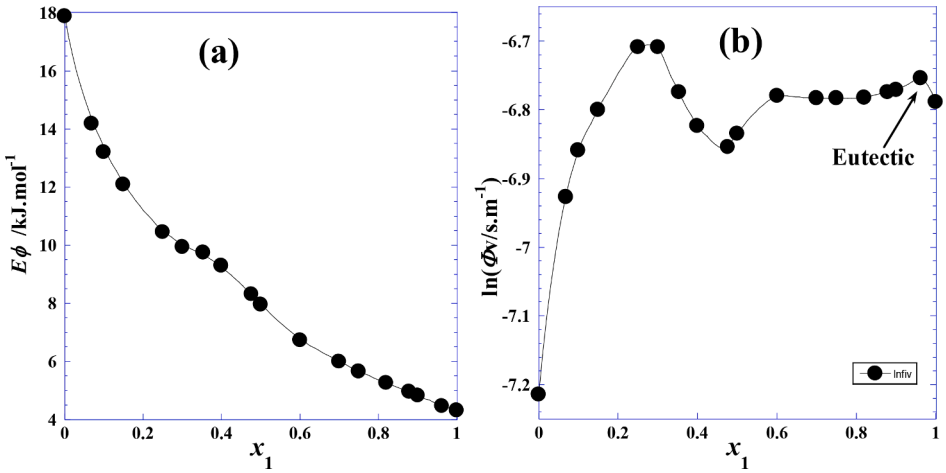

Fig. 18. Variation of (a): Friccohesity activation energy E_{φ} / (kJ·mol^{-1}) and (b): of the logarithm of pre-exponential factor ln(Φ_v/s·m^{-1}) of Eq. (23) for the {Sn (1) + Ag (2)} systems *vs.* the molar fraction (x_1) of Sn through the interval of temperature (623.15 to 1223.15) K.

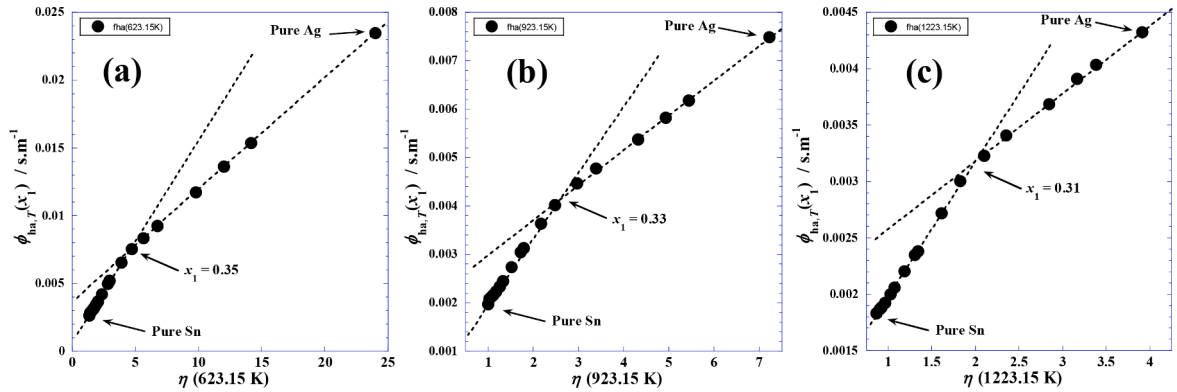

Fig. 19. Correlation between the apparent friccohesity φ_{ha} (s·m^{-1}) and the dynamic viscosity (η) of {Sn (1) + Ag (2)} systems at different molar fraction and fixed temperature. (a):623.15 K, (b): 923.15 K and (c): 1223.15 K.

Table 10
Surface tension's parameters values of Eq. 4 ($\sigma = \sigma_0 - S_\sigma \times T$) / N.m^{-1} for the {Sn (1) + Ag (2)} systems *vs.* the molar fraction (x_1) of Sn through the interval of temperature (623.15 to 1223.15) K.

system	Ref.	Range	σ_0	S_σ / 10^{-6}
Ag(2)	[66]	x_1=0	1.1489*	197.5
Ag(2)	Present Work	x_1=0	1.1640	204.0
Sn(1)-Ag (2)	Present Work	0< x_1<1	1.1371-1.3128x_1-3.6714 x_1^2+15.331x_1^3-17.087x_1^4+6.192x_1^5	197.75-1394.2x_1 +12259 x_1^2 -67189x_1^3 +1.8163e+5x_1^4 -2.4748e+5x_1^5 +1.6521e+5x_1^6 -43141x_1^7
Sn(1)	Present Work	x_1=1	0.63650	110.1
	[37]		0.59632*	89.775*

* The temperature range is not specified.

theory has explored a role on increasing Sn in the Sn+Ag alloys where the Ag could have acted as the doping agent similar to the Frenkel and Schottky defects that could have lowered the friccohesity. The increasing temperature has also favored more packing and Sn alignment around the Sn of the Sn+Ag alloy with comparative slightly stronger chemical adherence.

Furthermore, using linearization technique, our graphical manipulations of different physicochemical properties and its derived ones against temperature and composition reveal some spectacular and peculiar behaviors permitting us to suggest original empirical models interesting for prediction and estimation of new values using interpolation methods without resorting to experiments and thus making it possible to reduce the cost of essays. Likewise, we discovered that some derived properties reveal some particular compositions interesting for the study of the isobaric binary diagram through the peculiar compositions limiting some regions with different behaviors. The fundamental binding chemistry of the metallic constituents in the alloys in a specific stoichiometry has been a function of their individual binding or the cohesive energy as well as the conversion of the binding energies into the kinetic energies which had facilitated the individual kinetically active metallic atom to adhere around the core metallic atom which have been explained by the friccohesity chemistry.

The Sn-Ag binary alloy is one of the most common lead-free solders. So, it is characterized by more interesting thermo-physical properties. In the present work, we have suggested novel empirical expressions of these physicochemical properties against the temperature where the corresponding obtained optimal coefficients are expressed with mole composition of tin which permit us to combine the two dependences and propose unified equations correlating thermophysical properties of the alloy as the function of both the independent variables the temperature and composition.

In future works, it is aimed to generalize these novel findings to other interesting binary alloys in order to generalize to ternary and multi-components alloys.

Table 11
Density's parameters values of Eq. 5 ($\rho = a_{\rho 0} + a_{\rho 1} \times T$) / g.cm^{-3} for the {Sn (1) + Ag (2)} systems *vs.* the molar fraction (x_1) of Sn through the interval of temperature (623.15 to 1223.15) K.

system	Ref.	Range	$a_{\rho 0} = \rho_0$	$a_{\rho 1} = -\alpha \cdot \rho$ / 10^{-3}
Ag(2)	[66]	x_1=0	10.180	- 0.714
Ag(2)	Present Work	x_1=0	10.195	- 0.7278
Sn(1)-Ag (2)	Present Work	0< x_1<0.1	10.195-21.488x_1-107.18 x_1^2	
		0.1< x_1<0.4	9.107	
		0.4< x_1<1	339.64-3681x_1 +170889 x_1^2 -42860x_1^3 +62806x_1^4- 53924x_1^5 +25185x_1^6 -4947.7x_1^7	
		0< x_1<0.4761		-3.0668 -10.965x_1 +72.617 x_1^2 -378.85x_1^3 +376.16 x_1^4
		0.4761< x_1<1		619.55-4488.8x_1 +12278 x_1^2 -16256x_1^3 +10521x_1^4- 2680.2x_1^5
Sn(1)	Present Work	x_1=1	7.3101	- 0.6199
	[37]		7.118	- 0.507
	[67]		7.118	- 0.51

Table 12
Logarithm of viscosity's parameters values (lnη) of Eqs. 16, 17 and 18 for the {Sn (1) + Ag (2)} systems *vs.* the molar fraction (x_1) of Sn through the interval of temperature (623.15 to 1223.15) K.

system	Range	Equation	Logarithm of viscosity ln(η / Pa·s)
Ag(2)	x_1=0	17	$\ln\eta = -0.51621 + \frac{2303.1}{T}$
Sn(1)-Ag (2)	0< x_1<1	16 & 18	$\ln\eta = -0.51621 - 0.18115x_1 + \frac{2303.1 - 1649.55x_1}{T} - \frac{1288.05x_1(1-x_1)}{T - 145.7}$
Sn(1)	x_1=1	17	$\ln\eta = -0.69736 + \frac{650.55}{T}$

Author agreement statement

We the undersigned declare that this manuscript is original, has not been published before and is not currently being considered for publication elsewhere. We confirm that the manuscript has been read and approved by all named authors and that there are no other persons who satisfied the criteria for authorship but are not listed. We further confirm that the order of authors listed in the manuscript has been approved by all of us. We understand that the Corresponding Author is the sole contact for the Editorial process. Pr. Hicham Elmsellem is responsible for communicating with the other authors about progress, submissions of revisions and final approval of proofs Signed by all authors as follows:

Declaration of Competing Interest

The authors declare that they have no conflict of interest.

Acknowledgements

We state our deep gratitude and appreciation to Mr. Noureddine Ouerfelli, Professor at the University of Tunis El Manar, Tunisia, for his continued hold up all through the writing of this article.

Supplementary materials

Supplementary material associated with this article can be found, in the online version, at doi:10.1016/j.surfin.2021.101444.

References

[1] Directive 2002 95/EC of the European Parliament and of the Council of 27 January 2003 on the restriction of the use of certain hazardous substances in electrical and electronic equipment (ROHS).
[2] C. Schmetterer, E. C. in the F. of Scientific, and T. Research, COST 531 lead-free solders. 2. Handbook of properties of SAC solders and joints: ELFNET. COST office, 2008.
[3] I. Lauermann, G. Metzger, F. Sauerwald, Zeitschriftfür Physikalische Chemie (Leipzig) 216 (1961) 42.
[4] J.H. Vincent, B.P. Richards, D.R. Wallis, I.A. Gunter, M. Warwick, H.A.H. Steen, P. G. Harris, M.A. Whitmore, S.R. Billington, A.C. Harman, E. Knight, Circuit world, 19 (1993) 32.
[5] Z. Moser, W. Gasior, J. Pstruś, J. Phase Equilib. 22 (2001) 254.
[6] J. Lee, W. Shimoda, T. Tanaka, Mater. Trans. 45 (2004) 2864.
[7] R. Picha, J. Vřešťál, A. Kroupa, Calphad 28 (2004) 141.
[8] Z. Moser, W. Gąsior, J. Pstruś, A. Dębski, Int. J. Thermophys. 29 (2008) 1974.
[9] T. Gancarz, Z. Moser, W. Gąsior, J. Pstruś, H. Henein, Int. J. Thermophys. 32 (2011) 1210–1233, https://doi.org/10.1007/s10765-011-1011-1.
[10] S.J. Roach, H. Henein, Can. Metall. Q. 42 (2003) 175.
[11] S.J. Roach, H. Henein, Metallur. Mater. Trans. B 36 (2005) 667.
[12] P. Fima, Appl. Surf. Sci. 257 (2011) 3265–3268, https://doi.org/10.1016/j.apsusc.2010.11.002.
[13] T. Gancarz, W. Gąsior, H. Henein, Int. J. Thermophys. 35 (2014) 1725–1748, https://doi.org/10.1007/s10765-014-1748-4.
[14] E. Gebhardt, M. Becker, E. Tragner, Zeitschriftfür Metallkunde 44 (1953) 379.
[15] R. M'Chaar, M. El Maniani, M. El Moudane, A. Sabbar, J. Mater. Environ. Sci. 5 (2014) 2037.
[16] M. El Maniani, R. M'Chaar, M. El Moudane, A. Sabbar, J. Mater. Environ. Sci. 5 (2014) 2045.
[17] R. M'Chaar, M. El Moudane, A. Sabbar, A. Ghanimi, J. Theor. Comput. Chem. 15 (2016), 1650062, https://doi.org/10.1142/S0219633616500620.
[18] R. M'chaar, A. Sabbar, A. Ghanimi, M. El Moudane, J. Mater. Environ. Sci. 7 (2016) 4237.
[19] R. M'chaar, S. Belmoujoud, A. Sabbar, M.E. Moudane, A. Ghanimi, J. Theor. Comput. Chem. 16 (2017), 750015, https://doi.org/10.1142/S0219633617500158.
[20] R. M'chaar, M. El Maniani, A. Boulouiz, A. Ghanimi, A. Sabbar, M. El Moudane, J. Mater. Environ. Sci. 8 (2017) 1888.
[21] R. M'chaar, A. Sabbar, M. El. Moudane, A. Ghanimi, J. Theor. Comput. Chem. 16 (2017), 1750040, https://doi.org/10.1142/S0219633617500407.
[22] S. Belmoujoud, R. M'chaar, A. Sabbar, Surf. Rev. Lett. 26 (2019), 1950076, https://doi.org/10.1142/S0218625X19500768.
[23] R. M'chaar, A. Sabbar, M. El, Moudane, Sci. Rep. 9 (2019) 14177, https://doi.org/10.1038/s41598-019-50698-9.
[24] R. M'chaar, A. Sabbar, M. El. Moudane, N. Ouerfelli, Philos. Mag. 1 (2019) 1415–1438, https://doi.org/10.1080/14786435.2019.1704090.
[25] N. Dhouibi, A. Messaâdi, M. Bouaziz, N. Ouerfelli, A.H. Hamzaoui. Correspondence between Grunberg-Nissan, Arrhenius and Jouyban-Acree parameters for viscosity of 1,4-dioxane + water binary mixtures from 293.15 K to 320.15 K. Phys. Chem. Liquids. 50 (2012) 750–772. doi:10.1080/00319104.2012.717892.
[26] A. Messaâdi, N. Ouerfelli, D. Das, H. Hamda, A.H. Hamzaoui, Correspondence between Grunberg-Nissan, Arrhenius and Jouyban-Acree parameters for viscosity of isobutyric acid + water binary mixtures from 302.15 K to 313.15 K, J. Solution Chem. 41 (2012) 2186–2208, https://doi.org/10.1007/s10953-012-9931-3.
[27] M. Dallel, A.A. Al-Zahrani, H.M. Al-Shahrani, G.M. Al-Enzi, L. Snoussi, N. Vrinceanu, N.A. Al-Omair, N. Ouerfelli, Prediction of the boiling temperature of 1,2-dimethoxyethane and propylene carbonate through the study of viscosity temperature dependence of corresponding binary liquid mixtures, Phys. Chem. Liq. 55 (2017) 541–557, https://doi.org/10.1080/00319104.2016.1233181.
[28] M. Dallel, A.A. Al-Arfaj, N.A. Al-Omair, M.A. Alkhaldi, N.O. Alzamel, A.A. Al-Zahrani, N. Ouerfelli, A novel approach of partial derivatives to estimate the boiling temperature via the viscosity Arrhenius behavior in N,N-dimethylformamide + ethanol fluid systems Asian, J. Chem. 29 (2017) 2038–2050, https://doi.org/10.14233/ajchem.2017.20764.
[29] N.O. Alzamel, F. Alakhras, A.A. Al-Arfaj, M.A. Alkhaldi, N.A. Al-Omair, E. Al-Abbad, A.A. Wassel, N. Ouerfelli, On the homographic dependence of the activation energy and the viscosity Arrhenius' temperature for some pure fluids, Asian J. Chem. 30 (2018) 1937–1943, https://doi.org/10.14233/ajchem.2018.21319.
[30] E. Mliki, T.K. Srinivasa, A. Messaâdi, N.O. Alzamel, Z.H.A. Alsunaidi, N. Ouerfelli, Hyperbolic correlation between the viscosity Arrhenius parameters at liquid phase of some pure Newtonian fluids and their normal boiling temperature, Russ. J. Phys. Chem. A 94 (2020) 30–40, https://doi.org/10.1134/S0036024420010239.
[31] M. Singh, Survismeter – Type I and II for surface tension, viscosity measurements of liquids for academic, and research and development studies, J. Biochem. Biophys. Methods 67 (2006) 151–161, https://doi.org/10.1016/j.jbbm.2006.02.008.
[32] A Chandra, V Patidar, M Singh, RK. Kale, Physicochemical and friccohesity study of glycine, L-alanine and L-phenylalanine with aqueous methyltrioctylammonium

and cetylpyridinium chloride from T = (293.15 to 308.15) K, J Chem. Thermodyn. 65 (2013) 18–28, https://doi.org/10.1016/j.jct.2013.05.037.
[33] M Singh, V Kumar, RK. Kale, Viscous and surface properties of upper critical solution temperatures of immiscible solvents with biomolecules, surfactants and polymer resin, Int. J. Therm. 14 (2011) 87–95, https://doi.org/10.5541/ijot.345.
[34] RK Ameta, M Singh, RK. Kale, Synthesis and structure–activity relationship of benzylamine supported platinum (IV) complexes, New J Chem 37 (2013) 1501–1508, https://doi.org/10.1039/c3nj41141a.
[35] M Singh, V Kumar, JS Patel, RK. Kale, Thermodynamics of philicphobic interaction shift in aqueous Tweens 20-80, Int J Therm 14 (2011) 135–146.
[36] J.A.V Butler, The Thermodynamics of the Surfaces of solutions", Proc. R. Soc. London Ser. A, Contain. Papers Math. Phys. Character 135 (1932) 348–375.
[37] M. Kucharski, P. Fima, The Surface Tension and Density of Liquid Ag–Bi, Ag–Sn, and Bi–Sn Alloys, Monatshefte für Chemie 136 (2005) 1841–1846.
[38] Béranger G., Mazille H., Approche scientifique des surfaces. Caractérisation et propriétés, M1425, ed. Techniques de l'ingénieur. (2005) 1–21.
[39] N. Eustathopoulos, M.G. Nicholas, B. Drevet, Wettability at High Temperatures. Pergamon Materials Series, Elsevier, Amsterdam, 1999 vol.3.
[40] A.D. Kirshenbaum, J.A. Cahill, A.V. Grosse, The density of liquid silver from its melting point to its normal boiling point 2450 K, J. Inorg. Nucl. Chem. 24 (1962) 333–336.
[41] T.K. Rose. The precious metals, comprising gold, silver and platinum. D. Van Nostrand Company (1909).
[42] A.D. Kirshenbaum, J.A. Cahill, Trans. Am. Soc. Met. 55 (1962) 844.
[43] S.V. Stankus, R.A. Khairulin, The density of alloys of tin–lead system in the solid and liquid states, High Temp. 44 (2006) (2006) 389–395.
[44] E. Gebhardt, M. Becker, S. Schäfer, Z. Metallkd. 43 (1952) 292.
[45] E. Gebhardt, M. Becker, E. Trägner, Z. Metallkd. 44 (1953) 379.
[46] I. Budai, M.Z. Benkö, G. Kaptay, Mater. Sci. Forum 473–474 (2005) 309.
[47] T. Iida, R.I.L. Guthrie, The Physical Properties of Liquid Metals, Clarendon Press, Oxford, 1988.
[48] P. Terzieff, J. Alloys Compd. 453 (2008) 233.
[49] L. YaKozlov, L.M. Romanov, N.N. Petrov, Izv. vysch.uch.zav., Chernaya Metallurgiya 3 (1983) 7. Russian.
[50] A. Messaâdi, M.A. Alkhaldi, N.O. Alzamel, A.A. Al-Arfaj, F. Alakhras, A. H. Hamzaoui, N. Ouerfelli, An extended Belda equation for physicochemical properties correlation in binary liquid mixtures at different temperatures, Asian J. Chem. 1 (2018) 47–54.
[51] L. Grunberg, A.H. Nissan, Mixture law for viscosity, Nature 164 (1949) 799–800.
[52] W. Marczak, N. Adamczyk, M. Łezniak, Viscosity of Associated Mixtures Approximated by the Grunberg-Nissan Model, Int J. Thermophys 33 (2012) 680–691, https://doi.org/10.1007/s10765-011-1100-1.
[53] M.L.J. Kijevcanin, V.Z. Kostic, I.R. Radovic, B.D. Djordjevic, S.D. Serbanovic, Viscosity of binary non-electrolyte liquid mixtures: prediction and correlation, Chem. Ind. Chem. Eng. Quart. 14 (2008) 223–226.
[54] D.H. Alotaibi, E. Mliki, N. Vrinceanu, T.K. Srinivasa, M.E. Al-Oheli, A.A. Al-Arfaj, N. Ouerfelli, Validation of Messaâdi equation on viscosity-temperature dependence for some ternary liquid mixtures by statistical correlation analysis, Phys. Chem. Liq. 58 (2020) 590–602, https://doi.org/10.1080/00319104.2019.1625048.
[55] R. Hamdi, I. Massoudi, D.H. Alotaibi, N. Ouerfelli, Novel linear dependence between the viscosity Arrhenius parameters correlation in Newtonian liquids, Chem. Phys. 453 (2021), 111076, https://doi.org/10.1016/j.chemphys.2020.111076.
[56] A. Ali, AK. Nain, S. Hyder, Ion-solvent interaction of sodium iodide and lithium nitrate in N,N-dimethylformamide + ethanol mixtures at various temperatures, *J. Indian Chem. Soc* 75 (1998) 501–505.
[57] H. Eyring, M.S. John, Significant Liquid Structure, John Wiley & Sons, New York, NY, USA, 1969.
[58] Man Singh, Innovative Approach to Physicochemical Analysis, Publisher: I K International Publishing House Pvt. Ltd, 30 August 2020. First editionISBN-10: 9384588954, ISBN-13: 978-9384588953.
[59] Man Singh, Sunita Singh, Abdullah M.Asiri Inamuddin, IFT and friccohesity study of formulation, wetting, dewetting of liquid systems using oscosurvismeter, J. Mol. Liq. 244 (2017) 7–18.
[60] Rachna Gupta, Man Singh, Physicochemical properties of sustainable caped ZnO-Dendrimer nanocomposite with aqueous DMSO interfaces from 298.15–313.15 K, J. Mol. Liq. 322 (2021), 114936.
[61] O. Redlich, AT. Kister, Algebraic representation of thermodynamic properties and the classification of solutions, Ind. Eng. Chem 40 (1948) 345–348.
[62] J.E. Desnoyers, G. Perron, Treatment of excess thermodynamic quantities for liquid mixtures, J. Solution Chem 26 (1997) 749–755.
[63] D. Das, Shaik Babu, S. Slama, N.O. Alzamel, F. Alakhras, N. Ouerfelli, Investigation of Molecular Interaction in Benzene + Cyanex 923 Binary Mixtures at 298.15 K with Reduced Redlich–Kister Functions, Russ. J. Phys. Chem. A 93 (2019) 2669–2675, https://doi.org/10.1134/S0036024419130077. Issue 13.
[64] Shaik Babu, R. Trabelsi, T. Srinivasa Krishna, S. Mishra, N. Ouerfelli, A. Toumi, Reduced Redlich-Kister functions and interaction studies of Dehpa + Petrofin binary mixtures at 298.15 K, Phys. Chem. Liq. 57 (2019) 536–546, https://doi.org/10.1080/00319104.2018.1496437.
[65] R. Trabelsi, Shaik Babu, H. Salhi, N. Ouerfelli, A. Toumi, Investigations of the reduced Redlich-Kister excess properties of 1,4-dioxane + isobutyric acid binary mixtures at temperatures from 295.15 K to 313.15 K, Phys. Chem. Liq. 56 (2018) 801–815, https://doi.org/10.1080/00319104.2017.1399267.
[66] M. Kucharski, P. Fima, P. Skrzyniarz, W. Przebinda-Stefanowa, Surface tension and density of Cu–Ag, Cu–In and Ag–In alloys, Arch. Metall. Mater. 51 (2006) 389–397.
[67] E. Gebhardt, G. Wörwag, Die innere Reibung Flussinger Legierung ans Kupfer Silberund Gold-Kupfer, Z. Metallkd. 42 (1951) 358–361.